DOCTORAL THESIS

Development of methodologies to quantify spatial-temporal variability of arable crops for irrigation and fertilization management.

Lucía Quebrajo Moya

Universidad de Sevilla

Escuela Técnica Superior de Ingeniería Agronómica

2019

Thesis Supervisors:

Dr. Manuel Pérez Ruiz

Dr. Gregorio Egea Cegarra

Departamento de Ingeniería Aeroespacial y Mecánica de Fluidos

Development of methodologies to quantify spatial-temporal variability of arable crops for irrigation and fertilization management.

Memoria de tesis presentada por la Lda. en Geología, Dña. Lucía Quebrajo Moya para optar al Título de Doctora con Mención Internacional por la Universidad de Sevilla

Sevilla, Mayo 2019

VºBº del Director

Fdo. Manuel Pérez Ruiz

VºBº del Director

Fdo. Gregorio Egea Cegarra

Doctoranda:

Fdo. Lucía Quebrajo Moya

A mis padres, Andrés y Luisa

"It always seems imposible until it´s done"

— Mandela.

"En la vida no existe nada que temer, solo cosas que comprender"

— Marie Curie.

Acknowledgements/Agradecimientos

Llegado este momento, que parecía que nunca llegaría, me gustaría expresar mi más sincero agradecimiento a todas las personas que de uno u otro modo han hecho que este proyecto haya sido posible y que haya llegado a buen puerto.

En primer lugar, quiero dar las gracias a mis directores de tesis Dr. Manuel Pérez Ruiz y Dr. Gregorio Egea Cegarra por su inestimable ayuda, consejos, motivación, apoyo y aliento constante durante toda esta etapa.

Al Dr. Juan Agüera Vega, por su implicación en la primera parte de esta tesis y por estar siempre a mi disposición para cualquier consulta.

A mis compañeros en las salidas de campo, Jorge y Pablo, porque conseguimos sobrevivir a mil y una batallitas. Muchas gracias por el apoyo.

Quiero hacer una mención especial a la empresa Agrosap y a todos sus integrantes por “adoptarme” en mi etapa en Sevilla como una más de su gran familia. ¡Muchas gracias chicos!

Agradecer también a la Universidad de Sevilla por acogerme en esta última etapa de mi vida académica y a todas las personas que he conocido aquí y con las que he trabajado, porque he aprendido mucho de todos y cada uno de vosotros.

Mi sincero agradecimiento también para todos los compañeros de la Universidad de Florencia. Gracias por todo y por hacerme la vida más fácil allí. Grazie mille!

Me gustaría hacer una mención especial para mi amiga Claudia por su apoyo constante, por darme tanto ánimo incluso en los momentos más bajos y por creer en mí (casi más que yo) desde el principio. ¡Gracias amiga!

Y a mi amiga María y a toda su familia, por ser desde siempre parte de la mía y ahora aún más si cabe y sobre todo por estar para todo lo que yo he necesitado en esta etapa.

Por último, me gustaría dedicarselo a mi familia (Mamá, Papá, Marisa, Javier y Jesús) y a mis amigos por el apoyo e inyección de ánimo y moral durante toda esta aventura (Guía, Mercedes, Sonia, Pepa, Jorge y todos los que se puedan quedar en el tintero). A todos los que me han apoyado en cualquier momento de la travesía y en especial a los que ahora no van a poder verlo, porque estoy segura de que se alegrarían muchísimo.

CONTENTS

LIST OF FIGURES

Page

LIST OF TABLES

Page

ABBREVIATION LIST

ΔT	Temperature difference
ANOVA	Analysis of variance
CEC	Cation exchange capacity
CITIUS	Centre for research, technology and innovation at the University of Seville
CWSI	Crop water stress index
DANS	Degrees above non stressed
DGNSS	Differencial-global navigation satellite system
DOY	Day of the year
EC	Electrical conductivity
ECa	Apparent soil electrical conductivity
ECa_{25}	Apparent soil electrical conductivity at 25ºC
EGNOS	European geostationary navigation overlay service
ET_0	Reference evapotranspiration
FWHM	Full width at half maximun
GNSS	Global navigation satellite system
GPS	Global positioning system
HCP	Horizontal co-planar
IDW	Inverse distance weighting
LCD	Liquid crystal display
LEDs	Light-emitting diodes
N	Nitrogen
NDICEA model	A tool to improve nitrogen use efficiency in cropping systems
NDVI	Normalized difference vegetation index
NIR	Near infrared
NWSB	Non-water-stressed baseline
OM	Organic matter
PA	Precision agriculture
PrP	Perpendicular
QUEFTS model	Quantitative evaluation of the fertility of tropical soils
R	Soil moisture content
RDS	Radio data system
REW	Relative extractable water
R_{max}	Soil moisture content at the field capacity
R_{min}	Soil moisture content at the wilting point
RTCM	Radio technical commission for maritime services
SD	Secure digital
Ts	Surface temperature
UAV	Unmanned aerial vehicle
VIs	Vegetation indices
VPD	Vapour pressure deficit
VRA	Variable rate application
WS	Water-stressed conditions
WS_{Clay}	Water-stressed clay
WSI	Water stress integral
WS_{Sand}	Water-stressed sand
WW	Well-watered conditions
WW_{Clay}	Well-watered clay
WW_{Sand}	Well-watered sand

ABSTRACT

Growing concern about the role of agriculture in the sustainable management of natural resources (water, land and atmosphere), combined with the need to meet global food demand, creates an immediate need to improve production systems. Converting agricultural biosystems into highly efficient, economically profitable and sustainable productive elements requires the adoption of technology and the use of truthful, repeatable and actionable data.

In recent years, important technological advances including global positioning systems (GPS), yield monitors, variable rate technologies (VRT) and other sensors are already being applied and implemented in the field. This technology is being incorporated into crop production at all stages: sowing, fertilizing, pest and weed control, irrigation, harvesting, etc., so as to obtain the maximum information possible from each of them and enable a precise site-specific management.

Advances in different strategies and decisions that are taken daily in production systems are key to obtain maximum profitability at the lowest possible cost, which is the main objective of any producer.

The main objective of this doctoral thesis is to develop new site-specific information methodologies to characterize the spatial and temporal variability in key soil and crop traits in two herbaceous crops of high economic importance in Andalusia, autumn sowing sugar beet and winter durum wheat. Since sugar beet is an irrigated crop and durum wheat is normally a rainfed crop, this work has focused on the development of tools to optimize irrigation management of sugar beet and fertilization for durum wheat.

On the one hand, the feasibility of using an inexpensive and portable hand-held optical sensor for (1) estimating wheat yield response to N fertilization and (2) generating prescription maps of N application recommendations for commercial wheat fields has been evaluated. On the other hand, images captured with a

thermal imaging camera mounted on an unmanned aerial vehicle (UAV) were used to evaluate their potential to characterize the spatiotemporal variability of sugar beet water status when grown under heterogeneous soil and water management conditions.

Chapter 1: Introduction and Objetives

1.1. Background and rationale of the research

This thesis is organized into two research projects "Nuevas Estrategias Sostenibles para el Control de la Mala Hierba y Aplicación del Riego en Cultivos en Líneas mediante Técnicas de Agricultura de Precisión" (NESAP project, P12-AGR-1227, 2013-2016) and "Comparative study between applications of variable fertilization and conventional applications through the selection of the study plots, the corresponding sampling and the monitoring of the harvest" (FIUS: 2556/0332), carried out by the Smart Biosystems Laboratory (AGR-278) research team at ETSIA (Escuela Técnica Superior de Ingeniería Agronómica) of the University of Sevilla. The first project was funded by the Regional Government of Andalusia, and the second project was funded by a consortium of agricultural enterprises.

The world population, with approximately 7.15 billion people currently, increases by approximately 240,000 people every day. It is expected to reach 8 billion people by 2025 and 9.6 billion people by 2050. Almost all the potentially arable land is already being used and estimations say that food production must be increased by 70% by approximately 2050 if we want to feed the world population (CEMA - European Agricultural Machinery http://www.cema-agri.org/page/global-food-challenge).

An important drawback to achieve this objective is fresh water limitation. Only 2.5% of the existing water on Earth is fresh water, and of that, 0.5% is found in underground reservoirs and 0.01% in rivers and lakes. Therefore, only a minimal proportion of the Earth's existing water is usable to grow crops, and that amount is reduced year by year due to pollution and salinization of groundwater of arid zones. At the end of the 20th century, agriculture used on average 70% of all the water used and estimations indicate that irrigation will increase by 14 percent by 2030. By 2050, water consumption is projected to increase by 44 percent to meet industrial and population demands. Under this scenario, the United Nations (World Water Assessment Programme) warns that although there is enough water to meet the world's growing needs, it will not be possible if we don't radically change the way it is used, managed and shared. The

optimization of water use should, therefore, be one of the main concerns of agricultural scientists and stakeholders (www.fao.org / www.fundacionaquae.org). This is an unprecedented challenge to humanity, and there are many limitations to accomplishing such a feat. In Europe, the overall objective to cope with this challenge is to develop much-needed solutions to improve resource (e.g. water, nutrients) availability and to build more sustainable food production systems in a region heavily distressed by climate change, urbanisation and population growth (European Parliament - Science and Technology Options Assessment, 2nd. STOA Options Brief - Plant breeding and innovative agriculture; available at http://www.europarl.europa.eu/stoa/cms/home/events/workshops/feeding). To achieve this vital objective, the adoption of smarter farming methods, based on proximal and remote sensing, can provide new insights for optimizing agricultural processes.

The importance of this thesis lays in the development and assessment of precision agriculture methods for sugar beet and wheat, two relevant crops in terms of economy and cultivated land in some southern European countries, including Spain. Sugar beet was grown on 1.8 million hectares across the EU in 2017, whereas 310 million tonnes of cereals were produced in Europe in 2017 (Eurostat, 2018). In particular, Spain is the 8th largest EU sugar-producing country, with 3.5% of the total EU sugar beet area (1.5 million hectares). Andalusia produces nearly all the autumn-sown sugar beet in Spain. Sevilla stands out with 5,739.0 ha / 531,154.00 t and Cádiz with 2795.00 ha / 210,550.00 t of summer harvesting (data 2013/2014 campaign; https://www.mapa.gob.es/es/agricultura/temas/producciones-agricolas/cultivos-herbaceos/remolacha-azucarera/default.aspx). Spain is the 4th most productive EU producer of wheat, with 23.39 Mt, behind France (55.32 Mt), Germany (45.50 Mt) and Poland (30.24 Mt). When considering only winter wheat, the most productive countries are in the Mediterranean region, with Italy being the first producer, followed by southern Spain and Greece (Eurostat, 2018). In Spain, almost 100% of durum wheat production is concentrated between Aragon and Andalusia (MAPA

https://www.mapa.gob.es/es/agricultura/temas/producciones-agricolas/cultivos-herbaceos/cereales/).

In conventional agriculture, inputs are often distributed evenly throughout the field with the same amount of inputs applied per unit area. Best management practices for improving fertilizer and water use efficiency dictate the application location to maximize uptake, the best application dose to optimize growth, and the most appropriate material source (Drechsel et al., 2015). In principle, precision farming distributes inputs site specifically to gain marginal yield benefits from the same field or to conserve inputs. With a completely homogenous field (soil and crop), the potential benefits of site-specific application are in principle zero, but with heterogeneous fields, benefits are possible according to the variation in the yield potential or input saving potential from each field unit (Pedersen and Lind, 2017).

Presently, fertilizers (wheat) and water (sugar beet) are applied to fields uniformly and in quantities sometimes exceeding the amount required by the crops. This practice represents both a waste of natural resources and a source of environmental pollution. The application of variable rates of water and fertilizers has been proposed as a possible solution to optimize their use, and for this application, site-specific information on crop status and/or soil conditions is a prerequisite. However, although the availability of datasets on the existing within-field spatial variability is important (Bramley et al., 2011), it is even more important to derive procedures to convert the data into actionable information and use this information to determine the most economically efficient variable-rate input application practice.

1.1.1 Spatial variability of soil and crops

To transform conventional agriculture into smart agriculture, it is essential to determine the variability of soils (Miller et al., 1988; Schepers et al., 2004; Corwin and Lesch, 2005) and crops (Raun et al., 2005; Hall et al., 2008). Soil is one of the most important factors of agricultural production and can have a dominant effect on crop yields and quality (Eghball et al., 2003). The spatial-temporal variability in soil properties and crop yields has always been used in

conventional agriculture as an important aspect whose knowledge would allow for more efficient management practices. Precision agriculture (PA) involves optimizing small-scale inputs and managing spatial variability to obtain a general increase in profitability and environmental protection. PA contributes to sustainable crop production by reducing costs without lowering or even increasing production (reduced costs, optimized farm management, increased yields and higher quality harvests). The success of PA depends largely on highly efficient and reliable methods for collecting and processing site-specific field information.

The spatial variability of physico-chemical soil properties can be characterized by various sampling methods that, in combination with the use of global navigation satellite systems (GPS) and geostatistical tools (Goovaerts, 1998), allow the elaboration of soil variability maps that will later be used for the establishment of management zones (Moral et al., 2010). An example of the importance that knowledge of the spatial variability of soil and crop properties can have on farm management is that described by Arnó et al. (2012) in vineyards, who observed an inverse spatial correlation between grape yield and some grape quality parameters and showed that the percentage of carbonates in the soil had a great influence on grape quality.

Likewise, Martínez-Casasnovas et al. (2012) demonstrated that management zones defined from NDVI vegetation index maps are more effective in differentiating areas with different degrees of grape maturity and quality than those derived from yield maps.

1.1.2 Variable rate fertilizer and water application: Map-based system

The variable rate application of inputs, once the spatial variability has been characterized, can be addressed through two different approaches: map-based and real-time sensor-based systems. Map-based variable rate application adjusts the application rate based on an electronic map, also called a prescription map or application map (O'Shaughnessy et al., 2015). With map-based variable rate application, a GNSS receiver locates the applicator's

position on the map and the desired rate is then adjusted based on the prescription map as the applicator moves across the field (Grisso et al., 2011). Variable rate application of fertilizer implies that the mass flow rate and, subsequently, the application rate of fertilizer must be varied quickly as the applicator moves across the field. The spinner and pneumatic spreader are generally the most commonly used fertilizer application machinery, and fertilizer drills are frequently used. In general, the application rate is changed by changing the mass flow of fertilizer to the delivery system of the spreader (spinning disks or air boom). Current technology allows the rate between different swaths and in the longitudinal direction within one swath to be changed.

1.1.3 Variable rate fertilizer and water application: Real-time sensor-based system

While the map–based approach use historical information typically gathered with yield monitors, soil sampling and/or with data from sensors, the real-time sensor approach use real-time information gathered from sensors mounted on agricultural machinery to assess in–season conditions. The sensor–based approach therefore uses crop and/or soil properties measurements taken as the applicator moves across the field that are processed and interpreted by an on–board computer that is continuously sending control signals to a rate controller. The type of sensors used with this approach can be active or passive, with the predominant use of active sensors as they are unaffected by ambient light.

Within the active sensors, which emit their own source of light and measure the reflected light back to them, there are sensors that measure reflected light from different viewing angles, i.e. nadir or oblique angles. The sensors that have an oblique viewing angle are more suitable for crops in their early stages of development or in crops with higher plant spacing. This is the case, for example, of the sensors ‘N-Sensor’ (Yara UK Limited, Harvest House Europarc, Grimsby) and CropSpec (TopCon Corporation, Tokyo, Japan). On the contrary, the sensors that have a nadir viewing angle are more suitable for established crops or those with a higher density of foliage. This would be the case of the

Greenseeker (Trimble Navigation Ltd., Sunnyvale, CA, USA) and OptRx (Ag Leader Technology, Ames, IA, USA) sensors for variable rate application of nitrogen. Thermal infrared sensors, proposed for variable rate irrigation application by some authors (O'Shaughnessy et al., 2015), are flexible in this regard, having the possibility to be mounted with nadir or oblique viewing angles. Conversion of sensor readings into an application rate of any input (e.g. fertilizers or water in the case of travelling sprinkler systems) requires the use algorithms. These algorithms are simply equations that translate sensor readings into a signal (application rate) that the controller understands. A first step that must be always addressed with sensor-based variable application systems is to determine the relationship between the plant property of interest and the sensor readings. This is in many cases the main difficulty to be overcome, as the lack of this type of locally calibrated relationships for the crop of interest prevents the widespread of this type of methodologies.

With the data provided by these sensors, a nitrogen prescription is made taking into consideration an algorithm or formula, which can operate under different agronomic principles. The prescription in real time is calculated by means of a formula that considers the input information (by the user and the sensors). Different sensors are available to the production sector and have different operating principles, some of which are more suitable for use in certain growing conditions.

To measure soil moisture, real-time soil moisture sensors are used; these sensors are great tools that provide information on the moisture content in a soil profile. The important thing about these systems is that they carry out measurements in real time, providing the information needed to make irrigation decisions; this information is now sent over the Internet. The main disadvantage of these systems, from the point of view of the variable application of water, is that they are not remote sensors but must be installed in situ, so it represents a very expensive tool for the characterization of spatial variability. There are soil moisture probes in the market, such as the Profile Probe PR2 (Delta-T Devices, UK) or Diviner 2000 (Sentek Ltd., Australia), which are portable equipments that only require the permanent installation of access tubes where the probe will be

introduced manually to derive the soil moisture measurement. It is a cheaper alternative than having a probe measuring in real time at each specific site, however it has the cost of labor required to perform manual moisture measurement as main disadvantage.

Infrared thermography is a methodology that allows remote detection of water stress, not detectable visually, from the longwave radiation emitted by vegetation. Most of the energy absorbed by vegetation is dissipated in the form of latent heat of vaporization. When vegetation experiences some degree of water stress, the amount of energy dissipated by latent heat is reduced, increasing the temperature of the foliage. The use of infrared thermography to determine the water stress of the crop is based on quantifying the level of water stress that a plant has from temperature differences between a less-transpiring stressed plant and another that is transpiring at a potential rate.

These sensors can be used both for the determination of prescription maps for the application of irrigation and for irrigation management based on point sensors installed in certain specific sites of the plot. For the first option, thermal cameras represent a very powerful tool, especially when mounted on manned or unmanned aerial platforms. By means of image segmentation algorithms and subsequent processing of vegetation temperature data, maps of the spatial variability of the crop water status can be determined, which can in turn be transformed through a subsequent post-process operation in an irrigation prescription map.

1.2 Objectives

Based on the above information, the main objective of this doctoral thesis is to develop precision agriculture methodologies to characterize the spatial and temporal variability of key soil and crop traits in two crops of high economic importance in Andalusia, such as sugar beet and winter durum wheat. Since sugar beet is an irrigated crop and durum wheat is normally a rainfed crop, this work has focused on the development of tools to optimize irrigation management of sugar beet and fertilization of durum wheat.

This general objective has been divided into the following specific objectives:

Specific Objective 1: To determine the potential of the Normalized Difference Vegetation Index (NDVI), obtained by proximal sensing with an affordable hand-held active sensor, to estimate the spatial and temporal variability of leaf nitrogen content in wheat plants.

Specific Objective 2: To obtain NDVI-based empirical models to predict wheat yield as well as its spatial variability under the edaphoclimatic conditions of Andalusia.

Specific Objective 3: To develop variable rate fertilization strategies in commercial wheat fields based on either measured (yield monitoring) or estimated (NDVI-based statistical models) spatial variability of yield.

Specific Objective 4: To characterize the spatial variability of soils by means of electromagnetic induction sensors as well as the impact of the zones delimited by electromagnetic induction sensors on the sugar beet water status.

Specific Objective 5: To evaluate the use of thermal images taken from low-altitude drones to predict the spatiotemporal variations in sugar beet water status driven by soil variability and irrigation management.

Specific Objectives 1, 2 and 3 have been addressed in chapter 3 of this doctoral thesis, entitled "An Approach to Precise Nitrogen Management Using Hand-Held Crop Sensor Measurements and Winter Wheat Yield Mapping in a Mediterranean Environment". Specific Objectives 4 and 5 have been addressed in chapter 4, entitled "Linking Thermal Imaging and Soil Remote Sensing to Enhance the Irrigation Management of Sugar Beet".

1.3 Thesis structure and time-line

Figure 1.1 shows the structure of the thesis in terms of the different chapters, associated objectives, hypothesis and journals in which papers have been published. The main objectives of the thesis are addressed in the chapters 3 and 4, each of one corresponding to a scientific paper. Following the regulation of the University of Sevilla (Acuerdo 9.1/CG 19-4-12), which specifies the requirements for the thesis based on ‘compendium of articles’ format, each of

the focal chapters can be considered a self-contained unit. This means that they have an introduction section outlining the specific research context and objectives of the chapter, full details of the methods used, results, discussion and conclusions. The present chapter represents a general introduction of this thesis. Chapter 2 provides an overview of the methods used for the respective focal chapters. Finally, in chapter 5, a comprehensive discussion of the results obtained in focal chapters 3 and 4 is presented, allowing general conclusions to be drawn in relation to each of the objectives of the work. The general conclusions of the thesis are presented in chapter 6.

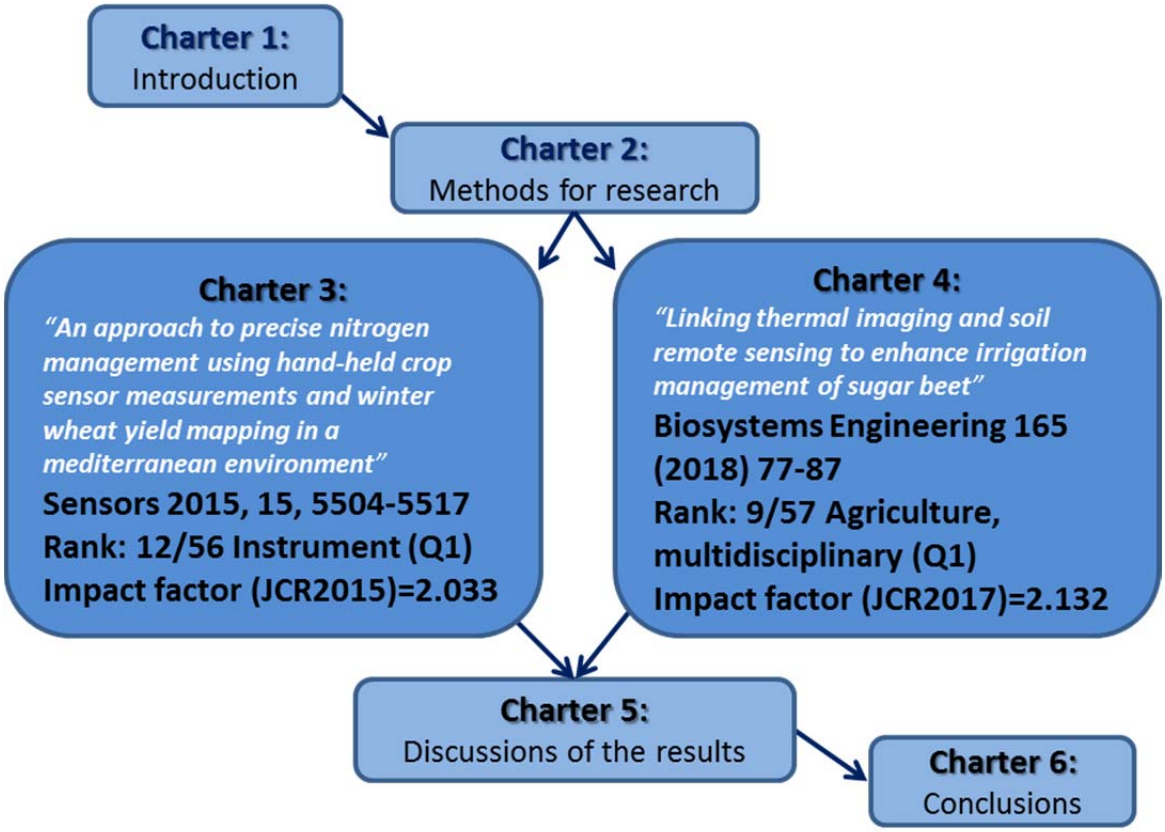

***Figure 1.1**: Thesis structure*

This thesis was performed within the framework of a 5-year doctoral programme (part-time candidate) financed partly by research projects at the University of Sevilla and by the doctoral candidate, from September 2014 to March 2019. The timeline of the different studies that comprise the thesis is shown in Figure 1.2.

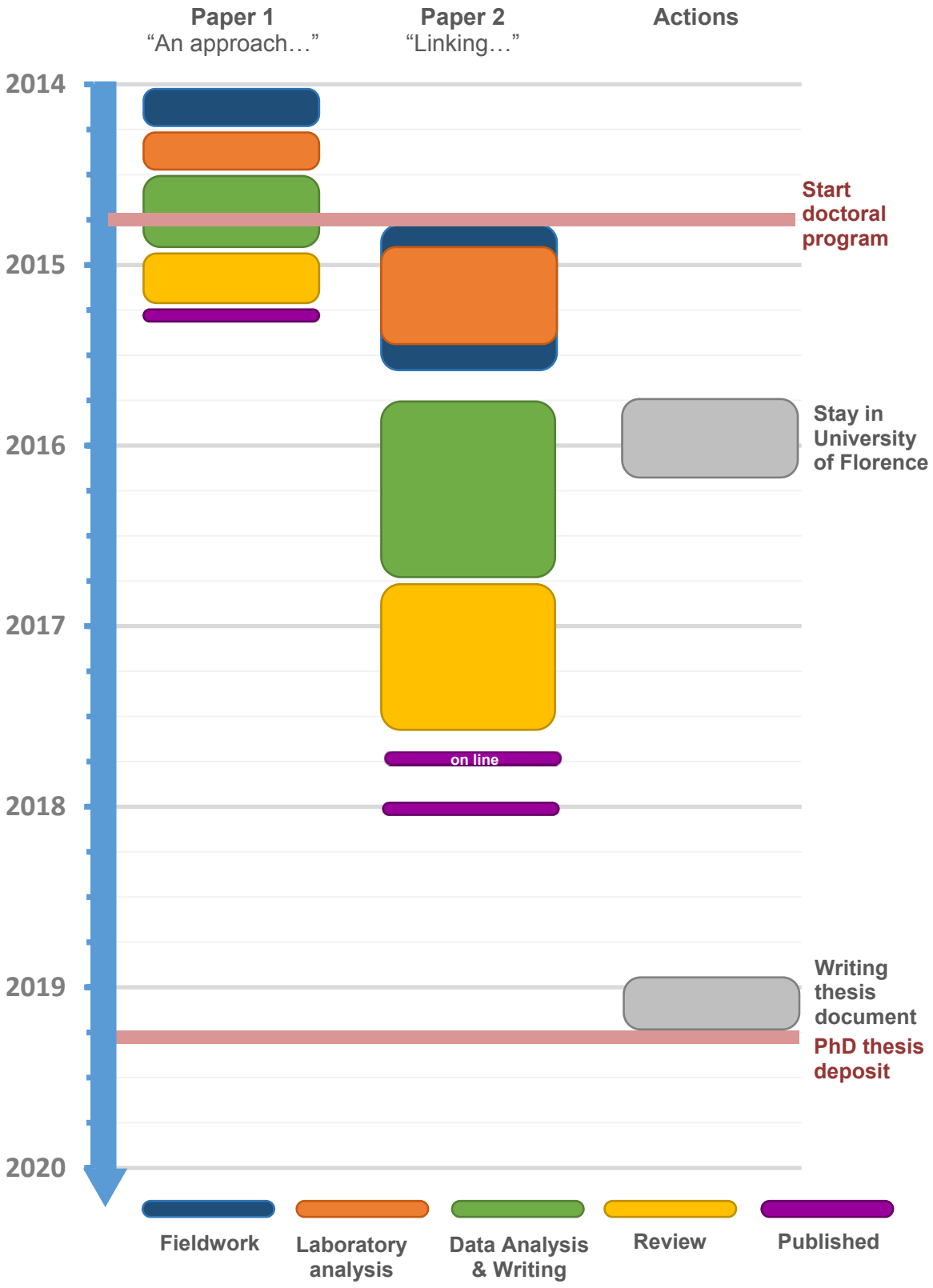

***Figure 1.2**: Timeline of the thesis*

Chapter 2: General workflow and short overview of methodology used for the research

2.1. Thesis workflow

Within the framework of the two main investigations carried out on both wheat and sugar beet, some sensors were used to measure soil and crop vigour variability. Finally, numerous sampling techniques and statistical procedures were carried out for different purposes using specific software and geostatistical methods and specific instruments for each of them.

2.2. Tests and instrumentation

2.2.1 Soil sampling, preparation and analysis

The sugar beet field used in this study was divided into a 60-m grid of approximately 0.36 ha/pixel. Thirty-one sampling points were selected within the grid for soil samples collection (Figure 2.1b). Soil samples were taken in October 2014, using an unaltered soil samples auger to a depth of 30 cm (Figure 2.1a), this being the depth of maximum root activity in a sugar beet plant.

The samples were collected in hermetically sealed bags until they reached the laboratory so that they would not lose moisture. The samples were weighed as soon as they arrived at the laboratory to obtain their fresh weight and subsequently dried in an oven (105ºC/48h) to determine soil bulk density and volumetric moisture content. The rest of soil analyses were performed at the Center for Research, Technology and Innovation (CITIUS laboratory) of the University of Seville, and the following parameters were analysed: pH, electrical conductivity (EC), oxidizable organic carbon (organic C), organic matter (OM), cation exchange capacity (CEC) and soil texture. Systematic sampling was performed by maintaining a fixed distance between two sampling points (using a net or mesh). All samples were georeferenced using a DGNSS (Differential-Global Navigation Satellite System) receiver and geographic information system (FarmWorks, Trimble Navigation Ltd., Sunnyvale, CA, USA) distribution maps of different soil properties compiled using a kriging technique (Goovaerts, 1997).

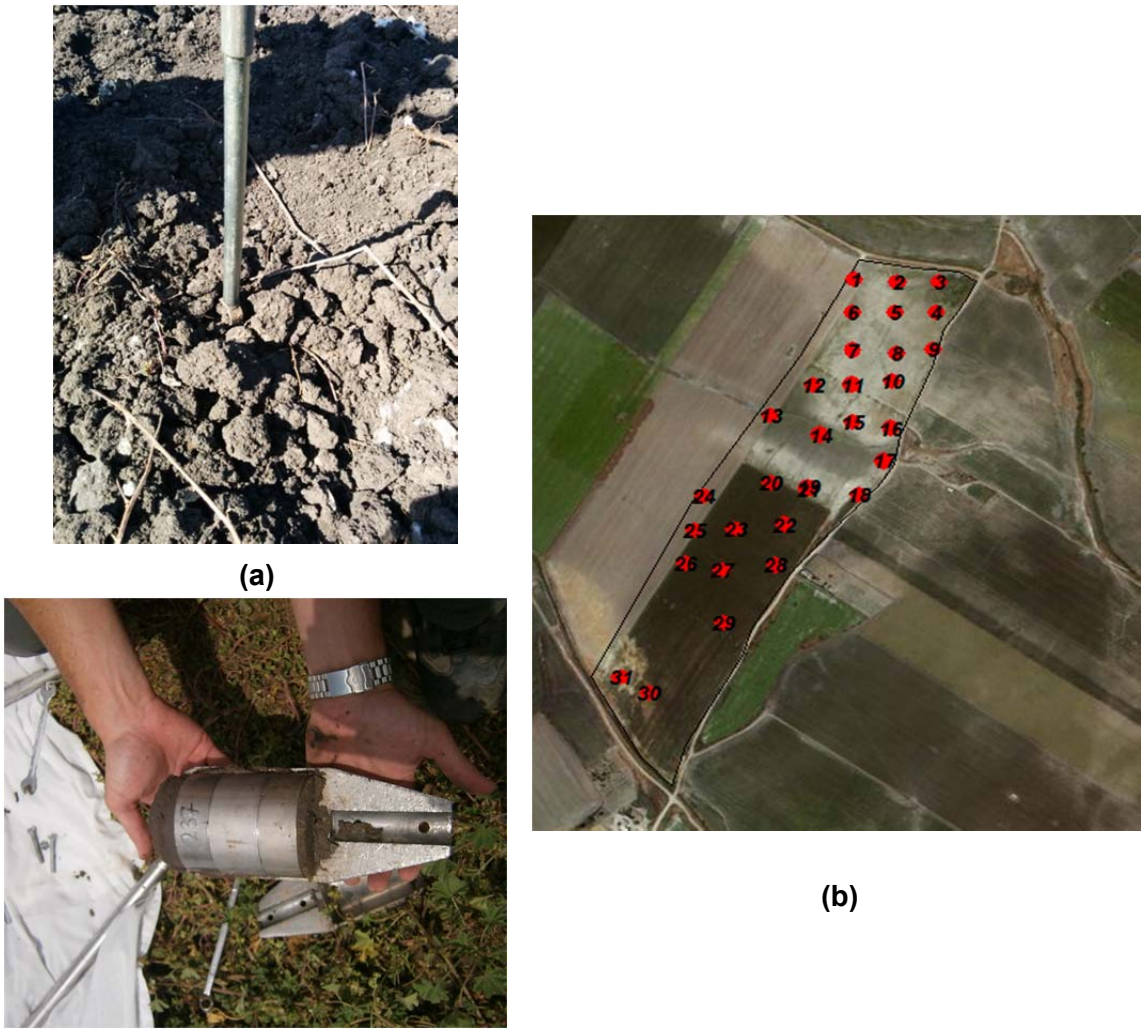

***Figure 2.1**: Soil sampling (**a**) and location of samples in the plot (**b**).*

2.2.2 Leaf N test

To determine the N content of wheat leaves, leaf sampling and laboratory analyses were conducted using the protocol of Mills and Jones (1996). The leaves were collected with care to manipulate them as little as possible and to avoid any loss of dry weight due to decomposition. Since no ears were apparent at the time of sampling, the highest (youngest) leaf was taken between leaves 4 and 5, which is the leaf that best defines the nutritional state of the crop (Mills and Jones, 1996). From each sampling location, approximately 50 leaves (one per wheat plant) were taken, carefully packaged in clean open paper bags and kept in a cool environment (5-7ºC) to avoid any N volatilization during the journey to the laboratory.

All the leaf samples were duly labelled and marked with their georeference, which was determined by means of a DGNSS receiver. The variability maps were elaborated with the help of GIS (Farm Works, Trimble Ag Software, Sunnyvale, CA, USA) by using the information from the samples and their georeferencing.

2.2.3 Beam-Based volumetric flow yield monitor

Yield, as a measure of the end product of most agricultural productive systems, is one of the most important datasets a producer can have. Commercial yield monitors currently available to farmers are based on a wide variety of measurement methods including a paddle wheel volume flow sensor (Searcy et al., 1989), a momentum plate sensor (Vansichen and De Baerdemaeker, 1991), a gamma ray sensor (Massey Ferguson, 1993), strain gage-based impact sensors (Borgelt, 1993), and an infrared sensor (Hummel et al., 1995). A grain yield monitor was designed to provide a real-time display of yield data and to estimate the weight of grain for a specified harvest area. Within the framework of this thesis, an optical grain yield monitor (RDS Ceres II, RDS Technology, Gloucestershire, UK) was mounted on a combine harvester (Claas-Mega 216, Claas Group, Harsewinkel, Germany). The combine, along with the yield monitor system, estimated the amount of wheat grain harvested from a specific area of the field, and this value was then attributed to a central point calculated by a GNSS receiver. This system consisted of a number of permanent sensors to measure yield, forward speed, moisture content, hill angle (2 axis) and header position (Figure 2.2).

The performance monitor measured the moisture and performance data, while the GNSS receiver used EGNOS to obtain location data with an accuracy of 3 m. Instant performance, humidity and GNSS data were recorded simultaneously at two-second intervals on a secure digital (SD) card installed on the performance monitor. The harvester had an effective cutting width of 6 m and travelled at an average speed of 4.5 km / h.

A light source was installed as high as possible on one side of the Ferris wheel of the combine, and on the opposite side a photosensor was mounted to

determine how much light could be detected from the source. Through this system, the height of grain contained in each bucket (Figure 2.2) was indirectly measured as the wheel went up (the higher the yield was, the greater the height of grain on each bucket and the less time the photosensor detected light when the bucket passed). By recording the time that the photosensor did not receive light, the computer transformed this time measurement into a value equal to the height of the grain on the bucket of the Ferris wheel. Then, the volume of grain was calculated by using the known surface area of the bucket.


(a)

(b)

***Figure 2.2**: Photoemitter and photosensor integrated in the buckets conduit to quantify crop flow (**a**) and Capacitive humidity sensor (**b**).*

2.2.4 On-the-go soil ECa mapping with Dualem 21-S

Apparent electrical conductivity (ECa) is a frequently used variable in precision agriculture (Corwin and Lesch, 2005). The apparent conductivity is influenced by a combination of physical-chemical properties so its value has been proposed to delimit the zones for variable rate application of inputs.

The main advantage of this method is the potential of the geophysical sensor to effectively characterize the soil spatial variability (moisture, organic matter, EC, etc) of a large sampling area in a short time (Pedrera-Parrila, 2014).

The ECa was measured using a Dualem 21-S EMI sensor (DUALEM, Milton, Canada) that operated 75 mm above ground protected in a polyvinyl chloride box and was pulled by an all-terrain vehicle (Figure 2.3) and coupled to a real-time differential global kinematic positioning system (Trimble, Sunnyvale, CA) to

collect samples on a 12-hectare strip of land. The sensor operated at a fixed frequency of 9 kHz.

Figure 2.3 *Dualem 21-S sensor working in the field.*

Measurements were collected in parallel rows spaced 10 m apart from NE to SW with the aid of a guidance system; points within a row were separated by 1-2 m. We also collected samples along 23 rows from NW to SE to increase the sample density.

The application of this technique consists of a system formed by coils or solenoids (emitters and receivers that generate a magnetic field when the current circulates through them) and a conductive medium (which in this case was the ground). The Dualem-21S allows up to 8 simultaneous measurements, 4 "in phase" (magnetic susceptibility) and 4 "out of phase" (CEa), as it has a total of 5 coils with varied separations and orientations (Figure 2.4, Simpson et al., 2009) and allows exploration of different depths. The combination of coils in the perpendicular position allows a shallower measurement depth, and the combination of coils in the perpendicular position with greater separation gives the maximum depth of exploration.

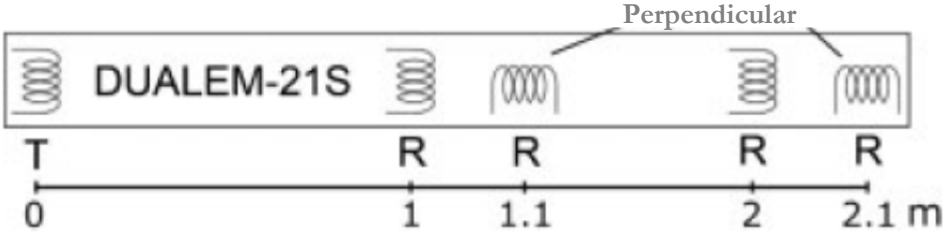

Figure 2.4 *Diagram of coil location and orientation in DUALEM-21-S (Simpson et al., 2009).*

The device consisted of a transmitter coil at one end and four receiver coils that were separated from the transmitter coil by 1, 1.1, 2 and 2.1 m. The receiver coils were oriented in a perpendicular (PrP) or horizontal co-planar (HCP) configuration with respect to the transmitter coils. Each combination of transmitter and receiver provided integrated ECa values for the corresponding volumes of soil scanned; these values depended on the scanning depth of each signal. The effective depth of exploration is the depth over which an array accumulates 70% of its total sensitivity, which also depends strongly on the soil ECa (Callegary et al., 2007).

The theoretical exploration depths for the combinations of 1.1 and 2.1 m HCP and the 1 and 2 m PrP coils were 0.5, 1.0 and 1.6 and 3.2 m, respectively. At high real conductivity values, the sensor has a non-linear response, and the ECa is increasingly underestimated for a given frequency and intercoil spacing (McNeill, 1980). Beamish (2011) proposed a correction procedure involving a polynomial of least-squares adjusted to the theoretical deviation of the linear relationship between the LIN-approximated ECa and the actual conductivity of the coil configurations to allow correction of the LIN approximation breakdown. This approach was adopted in this study, and the corrected approximate LIN ECa is used below. The coefficients used for polynomial adjustment are available in Delefortrie et al. (2014). The final transformation applied to the raw ECa data accounted for the soil temperature effects. A reference temperature of 25°C is generally used (Corwin and Lesch, 2005):

$$\mathrm{ECa}_{25} = \mathrm{ECa}\left[0.447 + 1.4034\mathrm{e}^{-\left(\frac{\mathrm{T}}{26.815}\right)}\right] \qquad (2.1)$$

where ECa25 is the standardized ECa at a temperature of 25ºC, and T is the soil temperature in ºC. To simplify the nomenclature, ECa is used as the temperature-corrected ECa reading (ECa25).

The average soil temperature was used at a depth of 0-0.30 m, obtained from 30 samples collected across the field. Given the high correlations between signals observed in the field (correlation coefficients ranging from 0.90 to 0.94), the 1.1 HCP signal that best represented the rooting depth of the sugar beet crop was used. The FAO has established a range of maximum effective rooting depths for sugar beet, i.e. 0.7-1.2 m (Allen et al., 1998).

The ECa data were filtered to eliminate false errors and interpolated by ordinary block kriging into a 2x2 m grid to create maps for the four ECa signals using a geostatistical analyst at ArcGIS (ESRI, Redlands, CA). We used an anisotropic spherical model to fit the variogram with a lag size of 1.5 m, range of 75 m, sill of 1663 $(mS\ m^{-1})^2$ and 115º as its main direction. A cross validation of the interpolation yielded a root mean squared error of 6.5 $mS\ m^{-1}$.

2.2.5 Remote sensing and vegetation indices (VIs)

Remotely sensed imagery have multiple applications in agriculture as they can help to assess problems or potential problems with soil degradation (Dubovyk, 2017) or plant growth (Zhang et al., 2018). . In precision agriculture it has also demonstrated great potential for delimiting management zones for variable rate application in a way that accounts for variation in soil properties (Cilia et al., 2014). However, interpreting imagery can be challenging because spectral reflectance is impacted by many factors, including vegetation density, the concentration of pigments (e.g., chlorophyll, carotenoids), canopy structure, soil properties (e.g., water, oxidized iron, carbon content), solar intensity, solar elevation angle, atmospheric factors and optics of the remote-sensing platform (Müller et al., 2015). Vegetation indicies (VIs) are numeric values obtained from the combination of two or more reflectance values corresponding to different bands of the spectrum (Hall et al., 2002). In practice, different VIs can be used to assess temporal and spatial variability of crop traits (Huete et al., 2000).

The normalized difference vegetation index (NDVI) (Rouse et al., 1974) is one of the most commonly used vegetation indices and is expressed as follows:

$$NDVI = \frac{NIR-Red}{NIR+Red} \quad (2.2)$$

where NIR and Red represent the spectral reflectance in the near-infrared (>725 nm) and red (600-725 nm) regions of the spectrum, respectively.

The commercial portable hand-held device GreenSeeker® (Trimble Navigation Ltd., Sunnyvale, CA, USA) is an affordable, easy-to-use measurement instrument used to evaluate plant biomass/plant health (Figure 2.5b). The sensor emits brief bursts of red light at 660±12 nm and near-infrared light at 770±12 nm and collects the amount of each type of light reflected from plants, which makes the sensor independent of ambient illumination. Once the device trigger is pressed, the sensor displays the mean NDVI value on its LCD screen, which varies from 0.00 to 0.99. The intensity of the detected light is a direct indicator of the health of the crop, i.e., a plant will be healthier and more vigorous when the NDVI value is higher (Gutiérrez-Soto et al., 2011).

Following the manufacturer's recommendations, measurements were taken at a vertical viewing angle from a distance of 0.5-0.6 m above the crop to ensure accurate readings. The sensor's field of view is an oval that widens as the sensor's height above ground increases, and a completely randomized design of 30 field test zones was used to perform the NDVI measurements (Figure 2.5a).

A field computer (Juno 5D, Trimble Navigation Ltd.) was used to record the location, time, date, number of satellites and NDVI reading for each sample in the internal memory (Figure 2.5b). The differential satellite receiver uses the EGNOS (European Geostationary Navigation Overlay Service) correction signals from any source that transmits the signals in the format of the Technical Radio communication Commission for Maritime Services (RTCM).

Some of the advantages of this sensor over other sensors are that this high-quality optical sensor measures the vigour of a plant instantly by simply

activating a trigger, is convenient for manual use, is charged through a USB charging port, and the display is easy to read even under direct sunlight.

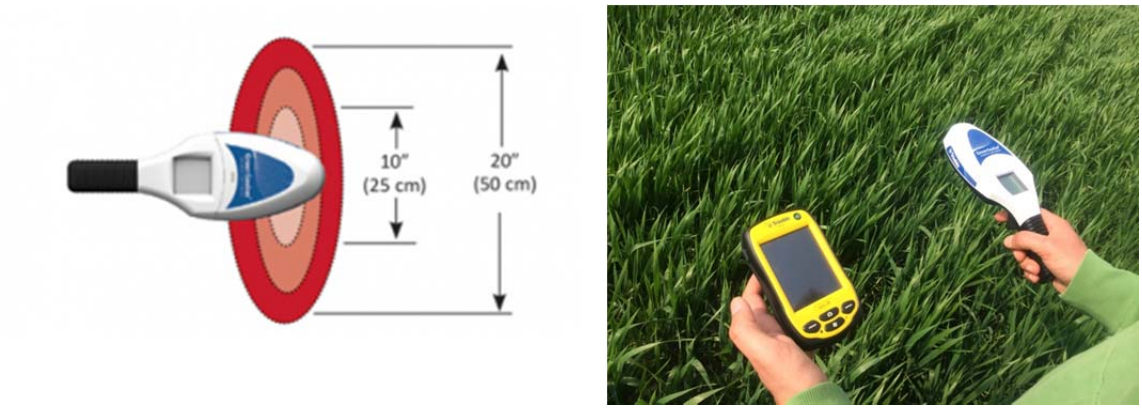

Figure 2.5 *The sensor's field of view is an oval (**a**). Hand-held NDVI sampling system in the experimental field (**b**)*

2.2.6 Soil moisture sensor

Soil moisture was measured in the 0-1000 mm soil profile during the study period using a multi-sensor PR-2 profile probe (Delta-T Devices, Ltd., Cambridge, UK). The advantage of this soil moisture probe is that it allows soil water profiles to be monitored with great ease and flexibility. The probe can be used in two different ways, (i) portable and (ii) fixed. In the first case, the probe is not left permanently installed inside an access tube, but is used to obtain point measurements at as many points as access tubes are available. In the second case, the probe is permanently installed in an access tube and can be used to monitor continuously the soil moisture profile at a single location

The PR2 soil moisture probe is a polycarbonate bar that has 6 sensors (6 pairs of stainless steel rings) that measure soil moisture content at 6 depths up to 100 cm (i.e. 10, 20, 30, 40, 60 and 100 cm) (Figure 2.6). The measurements are made inside an epoxy fibreglass tube with a rubber stopper that has previously been installed buried in the ground.

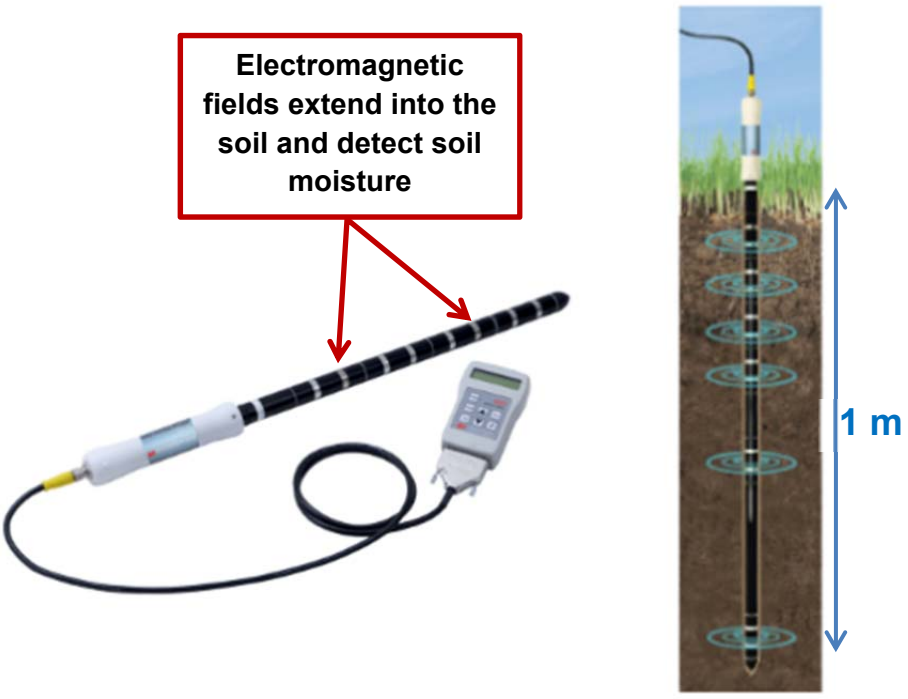

Figure 2.6 *Profile probe PR-2 (Source: https://www.delta-t.co.uk/product/pr2/).*

The PR-2 probe was calibrated for each one of the two selected zones for soil moisture monitoring; a sandy and a clayey zone, respectively. Calibration was performed following the manufacter's recommendations (Qi and Helmers, 2010), for which the coefficients of the linear equation used to convert the refractive index of the soil ($\sqrt{\varepsilon}$; ε being the soil permittivity) into volumetric water content were derived for each soil type. Calibration was carried out at the end of the sugar beet growth cycle, when it was possible to let the soil dry out and thus broaden the range of soil moisture conditions used to obtain the calibration coefficients. During the dry out period, unaltered soil samples were taken in the vicinity of the access tubes so that measured soil moisture contents could be related to the corresponding $\sqrt{\varepsilon}$ values measured with the PR-2 probe.

Soil samples were taken to the laboratory in duly labelled sealed bags. Once in the laboratory, gravimetric soil moisture values were determined for each soil sample by deriving their fresh and dry (after 48h/105ºC) weights. The dry soil bulk density was also determined for each soil sample by dividing soil dry weight by bulk volume (known value and equal to the volume of the cylinders of the unaltered soil samples auger). Volumetric moisture content was then calculated by multiplying gravimetric soil moisture contents by bulk density

(Verhoef and Egea, 2013). Once calibrated, soil moisture measurements in the 0-100 cm soil profile were used to calculate changes in relative extractable water (REW) for all experimental plots using the following expression:

$$\mathrm{REW} = \frac{\mathrm{R}-\mathrm{Rmin}}{\mathrm{Rmax}-\mathrm{Rmin}} \qquad (2.3)$$

where R is the soil moisture content, and R_{max} and R_{min} are the soil moisture contents at the field capacity and wilting point, respectively. The values for R_{max} and R_{min} were determined using the Rosetta model (Schaap et al., 1999), which is based on the van Genuchten model (Van Genuchten, 1980) and the physical properties of the soil measured in each selected zone.

2.2.7 UAV

An unmanned aerial vehicle (UAV) was used in the sugar beet experiment to carry a thermal camera used to take thermal measurements at plot scale. The model of the UAV used is a multi-rotor Phantom2 (SZ DJI Technology Co., Ltd., Shenzhen, China) equipped with a GNSS receiver whose main features are reflected in Table 2.1.

Table 2.1 *UAV technical data*

	UAV features
Weight (Battery & Propellers included)	1000g
Hover Accuracy (Ready to Fly)	Vertical: 0.8m Horizontal: 2.5m
Max Yaw Angular Velocity	200°/s
Max Tilt Angle	35°
Max Ascent / Descent Speed	Ascent: 6m/s; Descent: 2m/s
Max Flight Speed	15m/s (Not Recommended)
Diagonal Length	350mm
Flight Time	25mins
Take-off Weight	≤1300g
Operating Temperature	-10°C ~ 50°C
Supported Battery	DJI Smart Battery
Capacity battery	5200 mAh, 11.1V
Communication Distance to remote control (open area)	1000 m

This UAV has a multifunctional system of four rotors that allows a precise, safe and stable flight. The UAV has intelligent batteries that provide about25 min of flight autonomy, has a remote control range of 1000 m in open spaces and was controlled by the DJI iPad Ground Station application.It can automatically return home and land. The GPS with which the UAV is equipped is capable of tracking up to 12 satellites in the sky that help the pilot and are able to completely stall the device in the sky, even without the pilot touching the control. The GPS "locks" the drone in its current position and keeps it stationary.

2.2.8 Thermal sensor

A TAU 2324 thermal camera (FLIR Systems, Inc., Oregon, USA) mounted on a Phantom2 multi-rotor UAV (SZ DJI Technology Co., Ltd., Shenzhen, China) equipped with a GNSS receiver was used as a thermal sensor for this research. The accuracy of thermal measurements made with this type of camera mounted on a UAV has been reported to be approximately 1 K (Berni et al., 2009).

The camera was installed in a vertical orientation in the centre of the lower part of the UAV (Figure 2.7).

Figure 2.7 *Thermal camera mounted on UAV*

The flights were conducted on sunny days at solar noon. Thermal imaging was used to calculate the average sugar beet temperature in each experimental plot.

The UAV was flown across the experimental field on six days of clear sky during the period within the days of the year (DOY) 86 to 167. The flights measured the surface temperature over four selected experimental plots at various heights (5 m, 10 m, 20 m, 30 and 40 m) above ground level. The flight time over the different experimental plots and at different heights did not exceed 30-40 minutes (to minimize differences in weather conditions during the measurement period). The thermal images were acquired at a speed of 9 frames per second and were stored on board in a raw format with 14-bits radiometric resolution. A total of 50 selected thermal images per experimental plot were analyzed during the growth season.

The thermal images captured by the UAV were used to calculate the mean sugar beet temperature of each experimental plot by averaging the temperature of the pure vegetation pixels. Pure vegetation pixels were extracted from the thermal image using a segmentation algorithm written in R (R Core Team, 2015) and based on a histogram analysis of pixels from each thermal image and the "full width to half maximum" rule (FWHM). The FWHM rule allows the identification of pixels with a high probability of being pure vegetation, as described elsewhere (Rud et al., 2015; Käthner et al., 2017). In addition to the work scale, assessment of crop water status from thermal imaging is, against traditional leaf water potential measured with pressure bomb, a preferred and more informative option for many crops that present isohydric behavior, that is relatively steady leaf water potential values during water stress due to a strong stomatal regulation of water losses.

The assessment of crop water status was based on the difference between the average crop temperature and the prevailing air temperature at the time of flight (ΔT), measured using the air temperature sensor (model HMP45C Vaisala, Helsinki, Finland) installed at the nearby weather station (absolute accuracy of ±0.2ºC) belonging to the Agroclimatic Information Network of the Andalusia government (36º 43’ 08’’ N, 06º 19’ 48’’ W). The ΔT values can be used to assess differences in crop water status between plots if ΔT values are

measured under the same environmental conditions (e.g. solar radiation, vapor pressure deficit) (Maes and Steppe, 2012). In order to use ∆T to assess variations in crop water status throughout a multi-temporal series of thermal images, it is required to normalize ∆T values into an index of the type of CWSI described below. The ∆T values were also used to determine a cumulative water stress integral of the crop throughout the irrigation season. To accomplish this, an expression analogous to the water stress integral (WSI), originally proposed by Myers (1988) for predawn leaf water potential measurements, was used to determine the cumulative integral of water stress throughout the irrigation season:

$$\text{WSI (ºC day)} = \sum_{i=0}^{i=t}\left(\Delta T_{i,i+1} - C_{i,i+1}\right)n \qquad (2.4)$$

where t represents the number of measurements ∆T (t=6), in agreement with the number of flights conducted; $\Delta T_{i,\ i+1}$ is the ∆T average for any interval i, i+1; $C_{i,\ i+1}$ is the average of the non-water-stressed ∆T values for any period i, i+1; and n is the number of days in the interval. The c values were obtained from the non-water-stressed baseline (NWSB) derived by Idso (1982) to calculate the CWSI for sugar beet:

$$c_i = a + bVPD_i \qquad (2.5)$$

where VPD_i represents the prevailing vapour pressure deficit (kPa) at the time of flight on the i_{th} measurement day, and *a* and *b* are two parameters obtained empirically for each species under specific environmental conditions. The values *a* and *b* for sugar beet on sunny days are 2.50 and -1.92, respectively (Idso, 1982). The VPD and air temperature data at a height of 2 m were obtained from a nearby weather station belonging to the Agroclimatic Information Network of the Andalusia government.

The NWSB from IDSO (1982) was also used to calculate the CWSI of the i_{th} day of sampling as follows:

$$\text{CWSI} = \frac{\Delta Ti - ci}{\Delta T_{dry,i} - ci} \qquad (2.6)$$

where $\Delta T_{dry,i}$ represents the ΔT maximum, which corresponds to a non-transpiring canopy. In this case study, it was found that sugar beet leaf temperature could reach up to 8°C above the air temperature; consequently, a constant $\Delta T_{dry,i}$ = 8°C was used. Similar $\Delta T_{dry,i}$ values have been found for other herbaceous crop species (Rud et al., 2014).

2.3. Data Management

The data obtained with the different methods used in the various experiments carried out in this Doctoral Thesis were managed and analyzed with the help of geographical information systems and statistical methods.

2.3.1 Geographical Information Systems (GIS)

GIS are information systems capable of integrating, storing, editing, analysing, sharing and displaying geographically referenced information. In a more generic sense, GIS are tools that allow users to create interactive queries, analyse spatial information, edit data, draw maps and present the results of all these operations.

GIS operate as a geographic database associated with existing objects in a digital map, and respond to interactive queries of users by analysing and relating different types of information with a single geographic location, that is, connecting maps with databases. Basically, the functioning of a GIS goes through the following phases:

- Entry of information into the system (digital or pending digitalization)

- Storing and updating databases geographically, i.e., georeferencing information using latitude and longitude geographic coordinates.

- Analysis and interpretation of georeferenced data.

- Output of information in the form of different products depending on the user's needs.

GIS facilitate the work of the professional, since they separate the information in thematic layers and store them in an independent way, making the final task of relating the existing information to obtain results faster and easier.

The Agricultural Geographic Information System (Farm Works TM, Trimble Navigation Ltd., Sunnyvale, CA, USA) software package was used to facilitate the development of plans and maps that highlighted different features for the design of applications in the study area and to incorporate all the field data. The recorded data from the Juno 5D differential GNSS receiver were imported into the Farm Works TM software package to create different maps and applications. The inverse distance weighting (IDW) method implemented in the AgGIS (ESRI, Redlands, CA) software package was used for interpolation.

2.3.2 Data analysis

Once the data from all the trials were obtained, it was important before drawing conclusions to perform a statistical analysis using the R software package (R Core Team). R is a free software package for statistical computing and visualization that is distributed under the terms of the Free Software Foundation's GNU General Public License in source code form. This software is valued for its large variety of statistical methods and visualization capabilities.

In the statistical analysis, Pearson's coefficient, which is an index that measures the degree of covariance between linearly related variables and which ranges between −1 and +1, was obtained, and relationships between NDVI and wheat yield and NDVI and leaf N content were determined using the method of ordinary least squares.

Analysis of variance (ANOVA) were also performed with the statistical package Statgraphics (Statgraphics Centurion XV) and used to compare yield components and yield between treatments. The relationships between yield components and the water stress integrals were evaluated using linear regression analysis in Statgraphics software.

Chapter 3: Publication (I)

An Approach to Precise Nitrogen Management Using Hand-Held Crop Sensor Measurements and Winter Wheat Yield Mapping in a Mediterranean Environment

Lucía Quebrajo [1], Manuel Pérez-Ruiz [1,], Antonio Rodriguez-Lizana [1] and Juan Agüera [2]*

1 Aerospace Engineering and Fluids Mechanics Department, University of Seville, Ctra. Sevilla-Utrera km. 1, Seville 41013, Spain; E-Mails: lquebrajo@us.es (L.Q.); arodriguez2@us.es (A.R.-L.)

2 Rural Engineering Department, University of Cordoba, Córdoba 14071, Spain; E-Mail: jaguera@uco.es

Published in:

Sensors 2015, 15, 5504-5517

doi: 10.3390/s150305504

Received: December 29, 2014; Accepted: February 27, 2015; Published: March 6, 2015

Impact factor (JCR 2015): 2.033

Rank: 12/56 Instrument (Q1)

ABSTRACT

Regardless of the crop production system, nutrients inputs must be controlled at or below a certain economic threshold to achieve an acceptable level of profitability. The use of management zones and variable-rate fertilizer applications is gaining popularity in precision agriculture. Many researchers have evaluated the application of final yield maps and geo-referenced geophysical measurements (e.g., apparent soil electrical conductivity-ECa) as a method of establishing relatively homogeneous management zones within the same plot. Yield estimation models based on crop conditions at certain growth stages, soil nutrient statuses, agronomic factors, moisture statuses, and weed/pest pressures are a primary goal in precision agriculture. This study attempted to achieve the following objectives: (1) to investigate the potential for predicting winter wheat yields using vegetation measurements (the Normalized Difference Vegetation Index—NDVI) at the beginning of the season, thereby allowing for a yield response to nitrogen (N) fertilizer, and (2) evaluate the feasibility of using inexpensive optical sensor measurements in a Mediterranean environment. A field experiment was conducted in two commercial wheat fields near Seville, in southwestern Spain. Yield data were collected at harvest using a yield monitoring system (RDS Ceres II-volumetric meter) installed on a combine. Wheat yield and NDVI values of 3,498 ± 481 kg ha^{-1} and 0.67 ± 0.04 nm nm^{-1} (field 1) and 3221 ± 531 kg ha^{-1} and 0.68 ± 0.05 nm nm^{-1} (field 2) were obtained. In both fields, the yield and NDVI exhibited a strong Pearson correlation, with r_{xy} = 0.64 and $p < 10^{-4}$ in field 1 and r_{xy} = 0.78 and $p < 10^{-4}$ in field 2. The preliminary results indicate that hand-held crop sensor-based N management can be applied to wheat production in Spain and has the potential to increase agronomic N-use efficiency on a long-term basis.

Keywords: *NDVI; yield estimation; winter wheat*

3.1. Introduction

The goal of site-specific management practices is to enable more efficient use of fertilizers, pesticides, fuel, management and labor inputs. Most farming systems use spatial variability information related to crop status and soil characteristics to implement innovative management strategies to achieve a site-specific scenario. This new method of implementing agriculture is being bolstered by emerging cost-effective remote sensing techniques. Field crops must receive appropriate rates of nitrogen (N) fertilizer to achieve optimal yields; both underfertilization and overfertilization can negatively affect the desired growth pattern of plants and reduce yields. Furthermore, repeated machinery passes for N applications increase driving distances, require more time, increase soil compaction, consume more farming inputs and increase the environmental load (Oksanen et al., 2013).

Andalusia, in southern Spain, serves as an example of high agricultural value and represents 62% of the area (197,826.00 ha) used for and more than 80% of the national production of winter wheat, with an average yield of 3.11 t ha^{-1} (MAGRAMA, advancing production and area, July 2014). Using the average N fertilization application rate of 120 kg ha^{-1} per year and a price of 8–9 € ha^{-1} for application by a contractor company (two passes per fertilization) at 110 € t^{-1} of urea with 46% N amounts to a cost of 46.5 € ha^{-1} cost per year (fertilizer plus application). As much as 20% of inputs can be saved with the use of precision farming techniques and variable rate fertilizer application using proper machinery and precision application in areas with good yields and reduced inputs in areas with low yields (in which the lower yield may be due to soil limitations rather than insufficient N fertilization).

In this case, the cost would be 37.2 € ha^{-1} per year for the same yield at the end of the season. Andalusia could save approximately 1.8 M € using precision agricultural techniques for N application. Raun and Johnson (1999) reported that conventional N management strategies in world cereal production systems have resulted in a lower percentage of applied fertilizer N being recovered in the aboveground crop biomass during the growing season; they estimate that an average of only 33% of fertilizer N is recovered. Although it is impossible to

achieve 100% efficiency of N fertilizer use in any production system worldwide, the use of large amounts of N fertilizer suggests that there is a significant opportunity for reducing N losses associated with conventional practices.

Detailed knowledge of the relationship between applied fertilizer and crop yield in a zone under given soil conditions may be obtained through numerical approximations. Crop production models can be characterized as empirical and mechanistic (process-oriented) models. Empirical models directly employ a relationship between model variables and model outputs without requiring a description of fundamental (physical) processes. These models are usually site specific. Mechanistic models are often more complex because they describe known physical and biological processes in crops and soils. There are several models, such as the NDICEA model (Van der Burgt et al., 2006) that explore the relationship between applied N levels and their relationship to crop yield. The Quantitative Evaluation of the Fertility of Tropical Soils (QUEFTS) model, which is based on both theoretical and empirical relationships.

Janssen et al. (1990), showed that N applications improve crop yields (Liu et al., 2006), which is in agreement with the empirical results obtained by Wild (1992) and González-Fernández (2004) for wheat under various soil management systems. The use of these and other models may be of interest from an agronomic and environmental perspective because they improve on the traditional method of trial and error, which is more time consuming, and contribute to better decision making by farmers, thus resulting in savings in terms of fertilizer applied to the crop.

Remote sensing information is an integrated manifestation of the effects of on-field factors, such as soil texture, pH, biological and chemical factors, and of external factors, such as farming practices and weather conditions, on crop growth; therefore, remote sensing can have a substantial impact in improving yield estimation (Wheeler et al., 1996; Evans et al., 1997). Indirect sensing methods for measuring the ratio of vegetation indices (VIs) have been widely used to quantify crop variables such as yield and biomass; such methods may be available at different levels, depending on the type of platform that carries the imaging sensor, *i.e.*, satellite (Yang et al., 2006), aerial (Ballesteros et al., 2014) or ground (Stamatiadis et al., 2010) vehicles. Farmers who can distribute

the additional cost of improved management over a large operation can better absorb the high costs of satellite images (large-scale observation). Platforms that assess crop vigor cannot typically be used by small and mid-size agricultural operations because their costs can be very high and thus unprofitable for small-scale crops. The intrinsic drawback associated with satellite observations is the temporal frequency of satellite data. The degree of correspondence between the temporal frequencies of passive satellite remote sensor data collections and varying processes or crop statuses can significantly impact the accuracy of change detection monitoring efforts. Furthermore, the presence of clouds can reduce the number of opportunities for satellite data collection (Lunetta et al., 2004).

Small, unmanned aircraft systems and ground-based remote sensing hold great promise for small and mid-sized farmers because of their rapid development and decreasing costs (Peña et al., 2013; Wang et al., 2014). For ground-based images or the determination of VIs, an optical sensor with a computer recording sensor output may be mounted on the implement/tractor, or it may be used in survey mode (by hand); the global navigation satellite system (GNSS) field position is provided in both situations. The use of hand-held sensors can provide similar results at a much lower cost, which would make crops profitable and precision nutrient management (e.g., N) possible on small scales.

The spectral reflectance determined from image data has been used to calculate various Vis, such as the normalized difference vegetation index (NDVI), which is calculated by dividing the difference between the reflectances of the NIR and red bands by the sum of the reflectances of the NIR and red bands, *i.e.*, NDVI = (NIR − Red)/(NIR + Red). A variety of VIs, including reflectance band ratios and individual band reflectance, have also been used for crop management and yield prediction (Sobrino et al., 2000; Thomasson and Sui, 2009).

In terms of the N content, Tarpley et al. (2000) found that reflectance ratios calculated by dividing cotton leaf reflectances at 700 or 760 nm by a higher wavelength reflectance (755 to 920 nm) can provide accurate predictions of N concentrations. Furthermore, Shanahan et al. (2008) and Zarco-Tejada et al.

(2005) reported that N-status remote sensing is feasible for cereals and cotton, respectively.

The objectives of this work can be summarized as follows:

- To measure the NDVI of a winter wheat field under commercial management using a hand-held active remote sensing device and to determine the real wheat N content in collected leaf samples using laboratory analysis. The yield information (field level) will be obtained using a commercially available grain yield monitor.

- To determine the extent of spatial variability and co-variation between the wheat yield, N content and NDVI in two conventionally managed commercial fields used for wheat production.

3.2. Materials and Methods

This study was performed in two experimental plots (plot 1: 1.60 ha and plot 2: 1.21 ha) located in the western half of Andalusia (Southern Spain) in an area called the Countryside of Seville (Latitude: 37.4555477 N, Longitude: 5.4336677 W). The climate in this area is generally considered to be Mediterranean (summers that are dry and hot, low rainfall and strong evaporation demand). Typical crops in this area are arable crops and olive groves; therefore, we will study winter wheat because it is one of the most widespread crops in this area. In this case, the variety of wheat being grown is called COREL.

The soil is a vertisol, chromic haploxerert (Soil Survey Staff, 2014), formed on a Miocene marl. Clay is the predominant soil, with 64% in the 0–0.25 m layer, while sand makes up only 8% of the soil. The high carbonate content, 6.80%, results in a high pH value of 8.3. The available P content is 17.9 mg kg^{-1}, and the oxidizable organic matter is 1.65%. The ratio C/N is 9.82.

A typical wheat crop management scheme in this area consists of the following steps (and dates): basal fertilization on 22 December 2013; sowing on 24 December 2013; nitrogen fertilizer application on 3 February 2014; Herbicide treatment on 6 March 2014; fungicide treatment on 9 April 2014 and harvest on 5 June 2014.

3.2.1. Hand-held Optical Sensor and GNSS Control Unit

A commercial portable hand-held device (GreenSeeker®, Trimble Navigation Ltd., Sunnyvale, CA, USA) was used to measure the spectral NDVI of field-grown wheat leaves. The optical sensor emits a brief burst of radiation from red (Red; 660 ± 15 nm) and near-infrared (NIR; 770 ± 15 nm) light-emitting diodes (LEDs) to collect reflectance data that are independent of the solar conditions. The specific optical sensor was chosen because of its affordability and easy handling by field technicians and farmers.

The device measures the NDVI with a push of a button. The NDVI values range from 0.00 to 0.99. The liquid crystal display (LCD) provides the NDVI reading, with higher values indicating a more vigorous and healthy crop (Gutierrez-Soto et al., 2011). Following the manufacturer recommendations, measurements were taken at a vertical viewing angle from a distance of 0.5–0.6 m above the crop to ensure accurate readings. The sensor's field of view is an oval which, and it widens as the height of the sensor above the ground increases. A completely randomized design of 30 field-testing zones was used to perform the NDVI measurements.

A field computer (Juno 5D, Trimble Navigation Ltd.) was used to record the location of the technician at all times. This computer recorded the location, time, date, number of satellites and NDVI reading in the internal memory. The Juno 5D differential GNSS receiver utilizes a technology that combines a GNSS receiver, a differential beacon receiver and differential satellite receiver in the same housing. The satellite differential receiver uses EGNOS (European Geostationary Navigation Overlay Service) correction signals from any source that transmits the signals in Radio Technical Commission for Maritime Services (RTCM) format (Figure 3.1).

Figure 3.1 *Hand-held NDVI sampling system in the experimental field.*

3.2.2. Yield monitoring System

An RDS Ceres II yield monitoring system and an RDS GPS 16 receiver were installed on a Claas-Mega 216 combine harvester to estimate and record the yield and positional data, respectively. The yield monitor measured the moisture and yield data, whereas the GNSS receiver used EGNOS to obtain location data to within 3 m. The instantaneous yield, moisture, and GNSS data were simultaneously logged at two-second intervals onto a Secure Digital (SD) card installed on the yield monitor. The combine had an effective cutting width of 6 m and traveled at an average speed of 4.5 km/h. Therefore, approximately one sample was collected from a 15-m^2 area.

The optical sensor used to measure the grain yield was fitted onto the upper part of the clean grain conveyor just before the grain was dropped into the grain tank. An infrared light beam was transmitted across the elevator paddles from one side to the other. A receiver detected when the light beam was blocked and when it was clear. As each paddle passed the sensor, the beam was blocked. The more grain there was on the paddle, the longer the beam was blocked. The transmitter and receiver, together with their lenses and lens holders, were each secured to a hinged mounting bracket that was attached to the elevator housing. The sensor operation was indicated by an LED on the end of each sensor. Figure 3.2 presents the linkages and setup of the sensor.

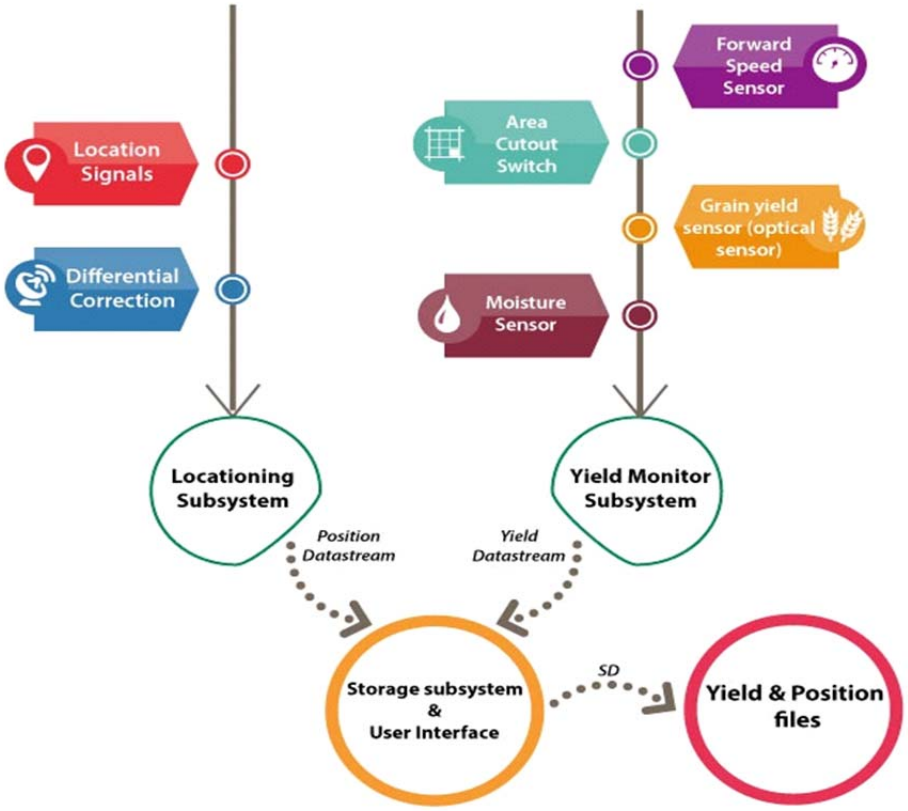

Figure 3.2 *A block diagram of the yield monitoring system components.*

3.2.3. Leaf N Test and Field Experiments

To determine the real wheat N content, leaf sample collection and laboratory analyses were conducted using the protocol of Mills and Jones (1996). The leaves were collected and specially handled to ensure that no loss in dry weight from decomposition occurred because such loss would significantly impact the plant analysis results. All the leaf samples were geo-referenced using a Juno 5D differential GNSS receiver; placed in open, clean paper bags; and kept in a cool (5–7 °C), environment during shipment to the laboratory to prevent N volatilization.

At the time of leaf sampling, ear emergence had not occurred; therefore, in accordance with Mills and Jones (1996), between the 4th and 5th leaf, the highest, *i.e.*, the youngest, leaf was taken because this leaf best defines the nutritional status of the crop. For each location sample, approximately 50 leaves (one per wheat plant) and 20 samples per field (two fields) were taken. Each field was homogeneous in terms of the soil and crop management. The N

content was determined at the CITIUS laboratory (University of Seville, Seville, Spain) using the LECO CNS-2000 instrument (LECO Corp., St. Joseph, MI, USA).

Field tests were performed during the spring of 2014 at a commercial wheat field (Latitude: 37.4555477 N, Longitude: 5.4336677 W). On 25 March 2014 (at the early growth), the NDVI measurements and leaf sample collection were obtained from two fields (1.60 ha and 1.21 ha). The NDVI values for each 350-m grid cell and the N percentage of leaves in 700-m grid cells within the study area were determined. On 2 June 2014, the harvest was conducted with the yield monitor system in place. The standard harvest procedures were slightly modified for calibration purposes to obtain accurate and completely site-specific yield information using the monitoring system.

3.2.4. AgGIS Software and Data Analysis

The Agricultural Geographic Information System (Farm Works TM, Trimble Navigation Ltd., Sunnyvale, CA, USA) software package was used to facilitate the development of plans and maps that highlighted different features for the design of applications in the study area and to incorporate all the field data. The recorded data from the Juno 5D differential GNSS receiver were imported into the Farm Works TM software package to create different maps and applications.

The inverse distance weighting (IDW) method implemented in the AgGIS software package was used for interpolation. It was assumed that spatial distribution variable, Z, decreased linearly (n = 1) with distance. The size of the neighborhood and number of neighbors are also relevant to the accuracy of the results (N = 12).

$$Zo = \frac{\sum_{i=1}^{N} z_i . d_i^{-n}}{\sum_{i=1}^{N} d_i^{-n}} \quad (3.1)$$

The variables in the above equation are the following:

Zo = the estimated value of the variable z at point i,

zi = the sample value at point i,

di = the distance from one sample point to an estimated point,

n = the coefficient that determines the weight based on a distance, and

N = the total number of predictions for each validation case.

Once the data from all the trials were obtained, it was important to perform a statistical analysis before drawing conclusions using the R software package (R Core Team, 2014). R is a free software package for statistical computing and visualization that is distributed under the terms of the Free Software Foundation's GNU General Public License in source code form. This software is valued for its large variety of statistical methods and visualization capabilities.

In the statistical analysis, Pearson's coefficient, which is an index that measures the degree of covariance between linearly related variables and which ranges between −1 and +1, was obtained, and relationships between NDVI and wheat yield and NDVI and leaf N content were determined using the method of ordinary least squares.

3.3. Results and Discussion

In Andalusia, Spain, the spatial statistical analysis of yield-monitored data has become relatively common for hand-harvested crops. This region is characterized by medium-large fields with homogeneous crops, and yield monitoring is often considered to be the main entry-level technology for use in precision agriculture. Spatial differences in wheat yields reflect differences in soil conditions that can, for instance, be repaired with fertilizer. These conditions are structural and are often reflected in the same patterns in the yields.

3.3.1. Yield Sensor Calibration and Yield Mesurement

Achieving accurate wheat yield measurements is challenging, and calibration effects the yield measurements. RDS Ceres operates with a light barrier in the upper part of the feed-flow side of the clean grain elevator. The grain piles on the elevator paddles interrupt the light beam. The zero tare value is obtained from the darkening rate when the elevator is running empty. Each day, taring was performed for both the combined yield sensor and moisture sensor. The

new calibration factor used in the yield monitoring in this study was calculated using the following, as proposed by Demmel et al. (2001):

$$\text{Calibration factor yield} = \frac{(\text{Existing factor} \times \text{Weight measured})}{\text{Weight from the console}} \qquad (3.2)$$

The mean relative error represents a measure of the calibration quality. It should ideally be zero, or at least near zero. In this study, the (average) relative calibration error was −3.1%, with a standard deviation of 4.2% (5 repetitions). This error was primarily due to the different specific weights of the wheat grains from different parts of the field. These values are very similar to those obtained by Demmel et al. (2013), with a mean of −0.14% and a standard deviation of 3.43%. Calibration is an important step for verifying the yield sensor output.

3.3.2. Relationship between the Wheat Yield and NDVI

The values of the wheat yield and NDVI for both fields were, respectively 3498 ± 481 kg ha^{-1} and 0.67 ± 0.04 nm nm^{-1} (field 1) and 3221 ± 531 kg ha^{-1} and 0.68 ± 0.05 nm nm^{-1} (field 2) (Figure 3.3). In both fields, the yield and NDVI exhibited a strong Pearson's correlation, with rxy = 0.64 and $p < 10^{-4}$ for field 1 and rxy = 0.78 and $p < 10^{-4}$ for field 2 (Figure 3.4). According to the categorizations by Dancey and Reidy (2004), these results denote a strong correlation between the yield and NDVI for both fields. The strong correlation suggests that NDVI measurements can be used for delineating management zones across a field, and such reliable and precise fertilizer (N) application has the potential to increase capacities in our agricultural environment. The visual similarity of the spatial distributions of the NDVI (Figure 3.5) and wheat yield confirms the close relationship between the two factors.

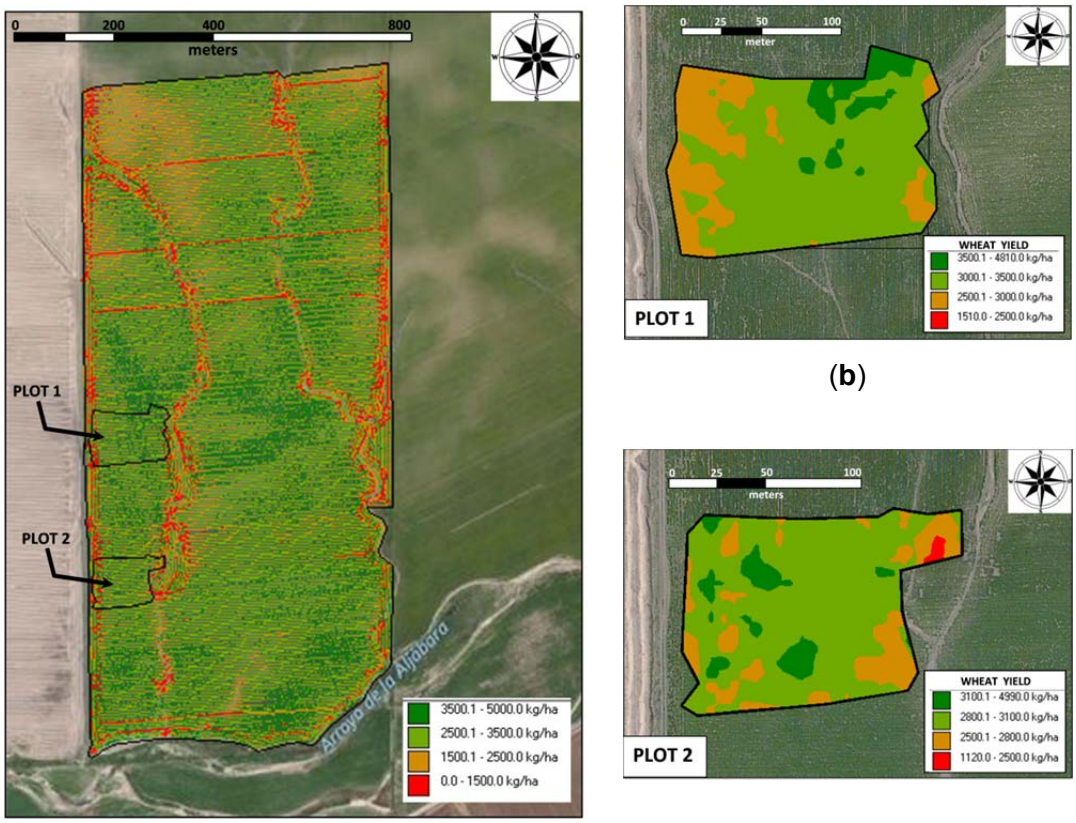

Figure 3.3 *(a) Map of the wheat yield and two NDVI sampling sites; (b) plot 1 and (c) plot 2.*

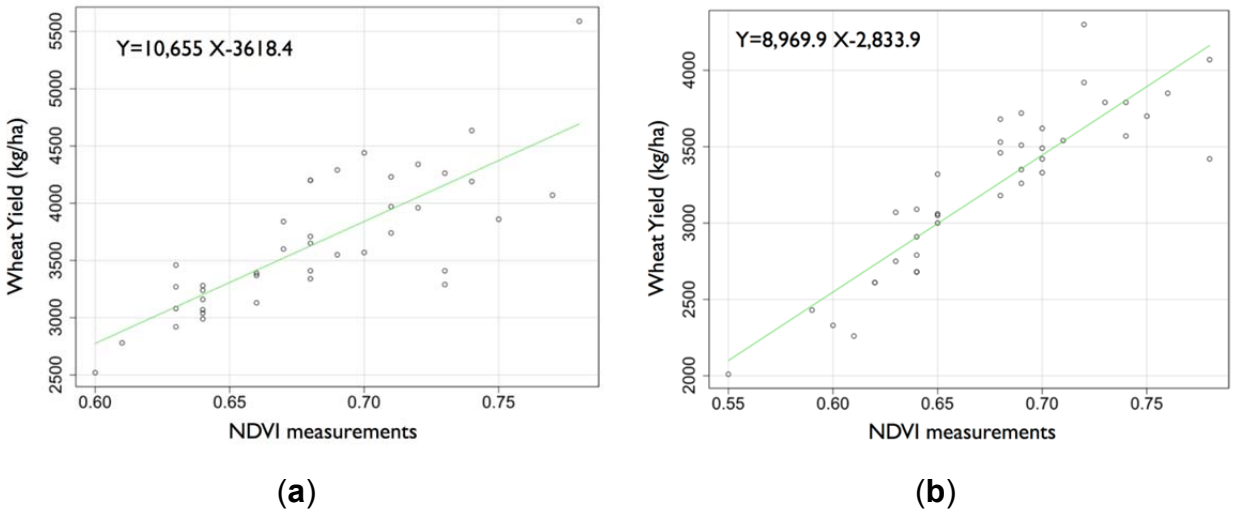

Figure 3.4 *(**a**) Relationship between the NDVI measurements and wheat yield (a) for field 1 and (**b**) for field 2.*

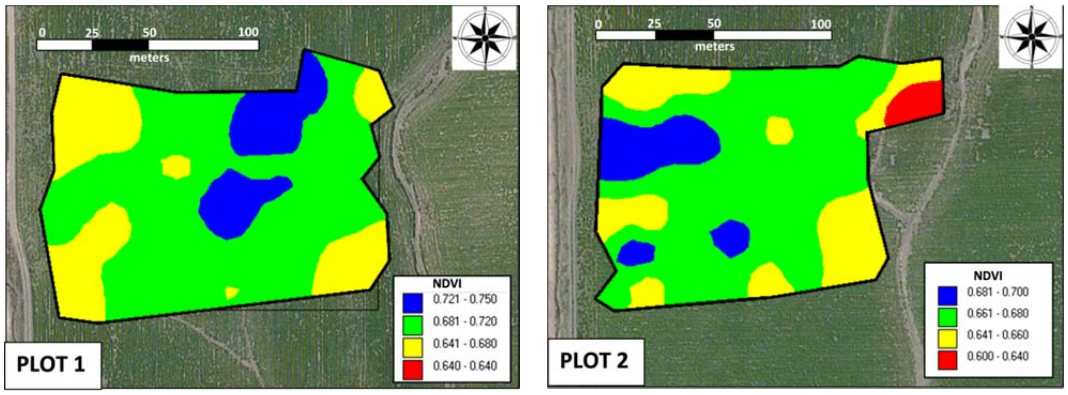

(**a**) (**b**)

Figure 3.5 *Spatial distribution of NDVI in both fields: (a) field 1 and (b) field 2.*

3.3.3. Relationship between Optical Sensor Measurements and Percentage of leaf N Content

Two field experiments were designed to determine the relationship between optical sensor measurement and the percentage of leaf N content. The measurements included 35 wheat leaf N content values (n = 17 for field 1 and n = 18 for field 2). The leaf N (%) values were 4.2% ± 0.44% (field 1) and 3.6% ± 0.24% (field 2). Figure 3.6 indicates a strong linear correlation between the N percentage content and NDVI measurements, which results in the following values: r_{xy} = 0.71 and $p < 10^{-4}$ for field 1 and r_{xy} = 0.89 and $p < 10^{-4}$ for field 2.

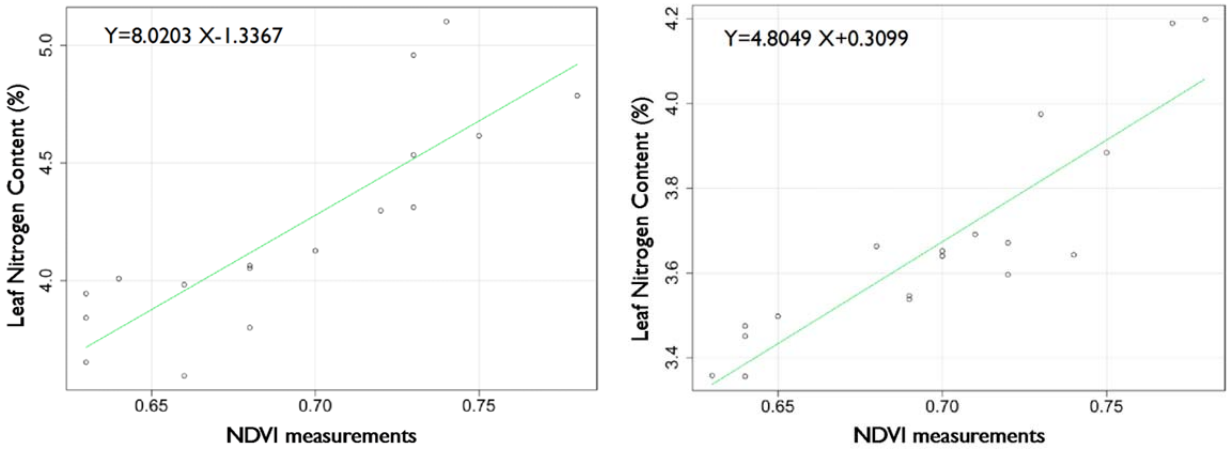

(**a**) (**b**)

Figure 3.6 *(**a**) The relationship between the NDVI measurements and leaf N content (a) for field 1 and (**b**) for field 2.*

3.3.4. Potential Value of Variable Rate N Application

A potential application of the NDVI sensor is to perform variable-rate N management for winter wheat, as shown in Figure 3.6. Currently, the method for determining the N (e.g., urea) requirements of wheat is to use the N-balance method; in some cases, estimation of the N application needed per hectare is based on the technician's and producer's experience.

In the same campaign and field, previous work evaluated N response tests with total N rates of 55, 150, 190, 225 and 250 kg ha^{-1} to determine the relationship between the NDVI measurements and total N. This relationship revealed a clear exponential regression in the measurements (r_{xy} = 0.99 and $p < 10^{-4}$). The exponential regression was as follows

$$y = 15.573e^{4.2795x} \quad (3.3)$$

where the variables are as follows:

y = Total N (kg ha^{-1})

x = NDVI sensor measurements

The use of optical sensors resulted in NDVI measurements that ranged between 0.60 and 0.78 in both fields. This information, along with the standard spatial interpolation method of IDW, allowed for variable-rate N prescription maps to be generated (Burrough and McDonnell, 1998). Figure 3.7 exhibits a preliminary approach to applying N at variable rates in fields to meet the predicted wheat N needs; however, it is important to note that the spatial patterns of optimum N rates for the same field can vary from year to year. According by Pedroso et al. (2010), for a field with precision farming, segmentation methods exist, and interest in such methods among researchers is increasing.

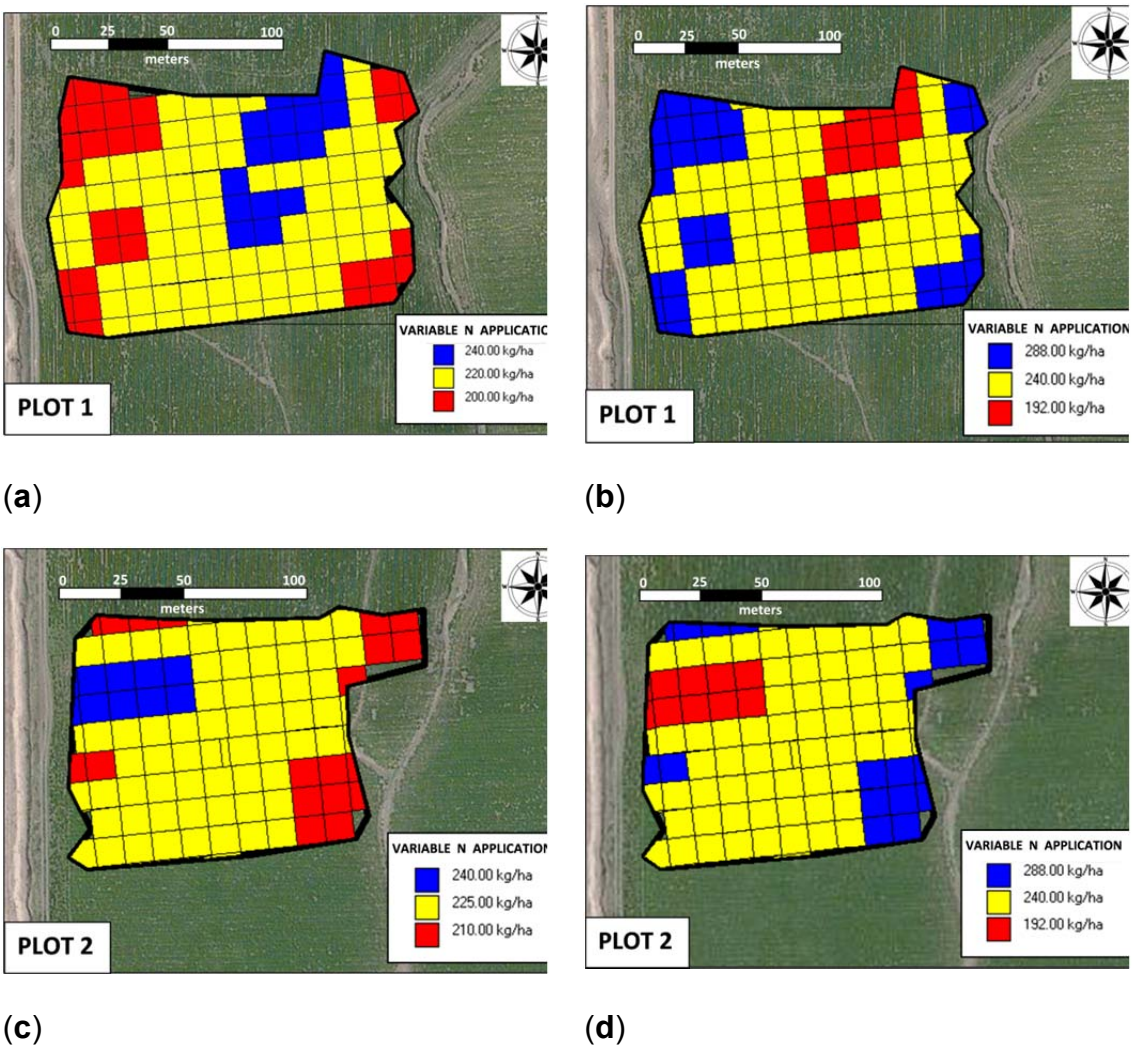

Figure 3.7 *Site-specific precise nitrogen management units for two fields: (**b**) and (**d**) conservative application, and (**a**) and (**c**) risky application.*

Figure 3.7 shows two theoretical farmer scenarios for variable-rate N application, conservative and risk taking, based on the number of N units to be distributed in the field. Usually, the farmer is reluctant to distribute fewer units than his experience would indicate are needed per hectare; therefore, a conservative scenario is necessary when the customary N units that are used in the area are distributed more in areas where higher yields are expected and less in areas with lower yield potential. With an average value of 240 kg N per hectare, Figure 3.7 b,d represent the conservative scenario; the average per hectare units are maintained to be equal to the rates that are used without precision farming tools (in Figure 3.7 b,d, max = 288 kg ha^{-1}, med = 240 kg ha^{-1}, and min = 192 kg ha^{-1}). The significant savings occur in the risk-taking

scenario, in which a producer decides to apply an average value of 240 kg N ha^{-1} in areas with the greatest potential and reduce the amount in areas with lower potential (in Figure 3.7 a, max = 240 kg ha^{-1}, med = 220 kg ha^{-1}, and min = 200 kg ha^{-1}; and Figure 3.7 c, max = 240 kg ha^{-1}, med = 225 kg ha^{-1}, and min = 210 kg ha^{-1}). The risk-taking strategy for variable-rate application of N reduce costs by approximately 20%. The risk taking strategy can be improved, for example, in cases in which the soil is the limitation to achieving higher yields.

All of maps shown in Figure 3.7 were generated on an appropriate grid (12 m × 12 m) using field positions from a GNSS receiver and a map of the desired application rate; the input rate changed as the spreader moved through the field. The N VRA (Variable rate application) machine should exhibit the highest real-time accuracy, but we observe that the mechanical nature of the application machine requires consideration of its limitations in the following areas: the working width (e.g., 12 m), minimum dose, maximum dose and time actuator settings. Another possible source of error is related to the characteristics of the applied material, e.g., the density and fluidity, which can change throughout the day; consequently, it is very important that the on-board equipment is well calibrated.

3.4. Conclusions

This ongoing research seeks new and improved tools to contribute to decision-making about the correct amount of N fertilizer to apply to winter wheat fields in a Mediterranean environment in a particular year. Until now, the adoption of VRA N management by producers has been very low, despite the potential economic and environmental benefits of this practice. Our major contributions are as follows:

The average percentage error of yield monitoring for detecting the actual mass flow rate was −3.1% with a standard deviation of 4.2%. This monitoring enabled an assessment of the relationship between the yield data and NDVI measurements (r^2 = 0.64 and 0.78) for fields 1 and 2.

An assessment of the relationship between the wheat leaf N content and NDVI measurements from optical sensor values revealed coefficients of determination greater than 0.9 when measured with the sensor.

An appropriate and inexpensive portable hand-held optical sensor (GreenSeeker®, Trimble Navigation Ltd., Sunnyvale, CA, USA) could satisfactorily help operators predict and generate a map of N application recommendations for fields. Wheat canopy greenness may not always be the result of a certain N content (e.g., available water or temperature may also affect the greenness). If the greenness is not related to the N content, then N inputs are based on an erroneous indicator.

- N recommendation maps were developed, and accurate N recommendations for sub-regions of fields were produced. The recommended N maps based on this technique may help operators use accurate and efficient application rates from year to year.

Acknowledgments

This study was supported, in part, by the project P12-AGR-1227 funded by the Regional Government of Andalusia. The authors want to express recognition to Salvador Correa at Soluciones Agrícolas de Precisión S.L. (Seville, Spain) and Francisco Javier Jiménez at Serfica S.L. (Carmona, Seville, Spain) for technical assistance.

Chapter 4: Publication (II)

Linking thermal imaging and soil remote sensing to enhance irrigation management of sugar beet

L. Quebrajo [1], M. Pérez-Ruiz [1,], L. Pérez-Urrestarazu [1], G. Martinez [2], G. Egea[1]*

[1] Universidad de Sevilla, Área de Ingeniería Agroforestal, Dpto. de Ingeniería Aeroespacial y Mecánica de Fluidos, Spain.

[2] Universidad de Córdoba, Dpto. de Agronomía, Spain.

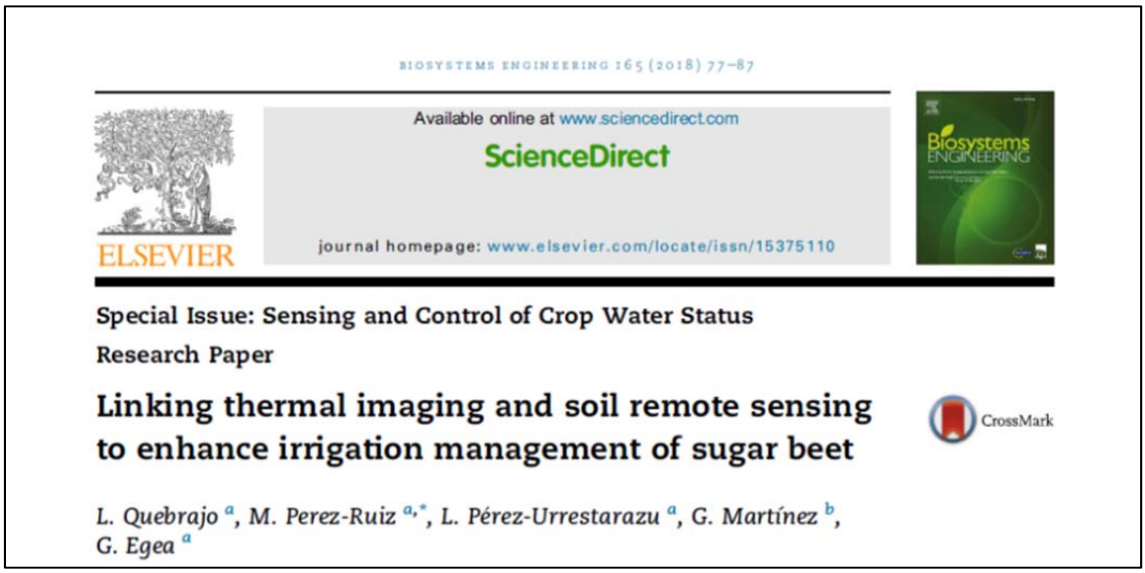

Published in:

Biosystems Engineering 165 (2018) 77-87

doi: https://doi.org/10.1016/j.biosystemseng.2017.08.013

Available online: September 2, 2017

Impact factor (JCR 2017): 2.132

Rank: 9/57 Agriculture, multidisciplinary (Q1)

ABSTRACT

The use of reliable information and data that are rapidly and easily acquired is essential for farm water management and appropriate irrigation strategies. Over the past decade, new advances have been made in irrigation technology, such as platforms that continuously transmit data between irrigation controllers and field sensors, mobile apps, and equipment for variable rate irrigation. In this study, images captured with a thermal imaging camera mounted on an unmanned aerial vehicle (UAV) were used to evaluate the water status of sugar beet plants in a plot with large spatial variability in terms of soil properties. The results were compared with those of soil moisture measurements. No direct relationship was observed between the water status of the soil and that of the crops. However, the fresh root mass and sugar content tended to decrease when higher levels of water stress were detected in the crop using thermal imaging, with coefficients of determination of 0.28 and 0.94 for fresh root mass and sugar content, respectively. Differences were observed between different soil types, and therefore different irrigation strategies are needed in highly heterogeneous plots.

Keywords: *Remote sensing, Unmanned aerial vehicle (UAV), Precision agriculture, Aerial image, Crop water stress index (CWSI)*

4.1. Introduction

Farmers, cooperatives and agricultural consultants are facing radical changes regarding the methods employed to collect, analyse, and use information to add value to their production outputs. Over the past 20 years, we have observed increasing interest in farm- and block-level precision agriculture (Blackmore et al., 2003; Zude-Sasse et al., 2016); however, the next 20 years will give rise to canopy-, branch-, and even fruit-level production practices that will demand a new farming mentality (Krishna, 2016). Field sensors will provide terabytes of quantitative and qualitative information about crops, such as nutrients levels and plant and soil moisture status, and about orchards, such as the three-dimensional canopy shape, the mass and size of each fruit, as well as the number of fruits per plant. Amassing this information into a coherent database that can be rapidly and easily used to make informed decisions on what, when, where, and how to plant, irrigate, prune, thin, treat and harvest each crop will soon be one of the fundamental challenges for farmers to address (Cox, 1996). This scenario allows farmers to move from intuitive decision making to analytical decision making.

Irrigation uses 70% of the freshwater (watercourses and groundwater) used worldwide, which is three times more than 50 years ago. During recent droughts, such as those in California (from 2013 to 2015) or Spain, continuous water deficits have increased from 15 to 60 months (López-Moreno et al., 2009); these droughts highlight the need for precision irrigation techniques to improve water use efficiency so that the resource is applied exactly at the right location, time and rate. The possibilities introduced by the use of remote sensing include precise water management within a plot. Therefore, different irrigation strategies can be followed based on the spatial variability of the soil and crop conditions. Because of this variability, the actual water requirements of crops may change within the same plot. In this case, the challenge for precision irrigation is the development of methodologies to acquire the required information that will allow uniform management within demarcated areas in the plots and the validation of protocols that enable precise irrigation in various sub-units.

Soil moisture monitoring through instruments placed in a few locations in a field has been argued to have important disadvantages that are primarily related to representativeness and the fact that crop water status depends on other factors in addition to soil moisture content (Jones, 2004). The water status of plant tissues, which is commonly measured in terms of water potential (Jones, 1992), can be used as a precise indicator for irrigation scheduling (Jones, 2004). Pressure chambers (Scholander et al., 1965) have been widely employed to measure leaf water potential for water deficit determination and irrigation scheduling. Although this method is a reliable measure of plant water status, it is highly time consuming and labour intensive, which results in inadequate sampling (Cohen et al., 2005). Moreover, this method is not feasible for measuring the water potential of certain leaf types, such as those of sugar beet.

Measurement of canopy temperature has been proposed as an alternative method of determining water potential (Bellvert et al., 2016). As water stress is induced, the stomata close, transpiration rates decrease and evapotranspirative cooling is reduced, causing leaf temperatures to increase (Maes and Steppe, 2012). Idso et al. (1981) and Jackson et al. (1981) suggested the use of the crop water stress index (CWSI) as an indicator of plant water stress. Sensing the canopy temperature using infrared sensors or imaging has shown good potential for calculating the CWSI and estimating the plant water status for irrigation scheduling in cotton, corn, sunflower, grapevine, and pistachios (Gonzalez-Dugo et al., 2006; Payero et al., 2006; Möller et al., 2007; Testi et al., 2008; Taghvaeian et al., 2014). Although a non-water-stressed baseline, i.e., a wet reference, to calculate the CWSI was reported for sugar beet (Idso, 1982), the upper baseline, i.e., a water-stressed baseline or dry reference, contains some uncertainty, with most studies assuming a rather arbitrary fixed temperature increment above air temperature to represent the temperature of non-transpiring leaves; values approximately 5ºC above air temperature are often used. Alternatively, the degrees above non-stressed (DANS) index, which is a simplified version of the CWSI that is based only on the difference between the stressed and non-stressed canopy temperatures, can be used (DeJonge et al., 2015; Taghvaeian et al., 2014). However, to the best of our knowledge,

thermal sensing has not been applied to optimize sugar beet irrigation. The sugar beet is considered a high water-consuming crop (Fabeiro et al., 2003), and its future in drought-prone areas with limited water resources could be compromised if crop productivity is not maintained under expected reductions in available irrigation water. To attain this objective farmers are obliged to implement precision irrigation tools, such as thermal-based crop stress sensing, which may overcome the drawbacks of soil moisture and leaf water status monitoring, especially when remotely monitoring large areas of crops.

The earth-emitted thermal energy is a function of the surface temperature (Ts) and the surface emissivity, where emissivity is a material property that ranges in value from 0 to 1 (Snyder and Wan, 1998). Since remote sensors can detect and quantify the heat emitted from the earth, the surface temperature can be easily determined. Thermal images captured using micro-unmanned aerial vehicles (UAVs) have considerable advantages over manual infrared thermometers, which require considerable effort and have low representation of measurements, and thermal imaging satellite data in which the spatial and temporal resolution is not sufficient for most irrigation applications. For small- and medium-sized plots, UAVs have a competitive advantage over large, autonomous aerial platforms, such as manned aircrafts carrying considerable amounts of remote sensing equipment.

The goal of this study was to evaluate the use of thermal images captured using a micro-UAV to predict variations in crop water use due to soil variability and irrigation management. This method can subsequently be used as a decision support tool for the efficient irrigation management of sugar beet.

4.2. Materials and methods

4.2.1. Field description and esperimental conditions

Field tests were conducted in a commercial sugar beet field (Beta vulgaris L., ssp. vulgaris var. altissima) during the 2014/2015 growing cycle (i.e., from October to July). The field was located in Cadiz, SW Spain (Latitude, 36.6965397º N; Longitude, 6.3184375º W). The experimental field covered an

area of approximately 12 ha and was irrigated with a sprinkler system consisting of a triangular arrangement of emitters spaced 12 m apart along the laterals; the laterals were also spaced 12 m apart. The sprinkler wetting radius was approximately 12 m at a working pressure head of 30 m. In southern Spain, sugar beet is sown in autumn. In the experimental field, the crop was planted in mid-November at a depth of 25 mm with 120 mm between plants and 500 mm between plant rows. The climate of the study area is Mediterranean, with rainfall occurring normally from late September to May. The average annual reference evapotranspiration (ET_0) and precipitation values calculated for the 2012-2015 period from data recorded at a nearby weather station belonging to the Agroclimatic Information Network of the Andalusia government (36º 43' 08" N, 06º 19' 48" W) were 1273 mm and 471 mm, respectively. Table 4.1 shows the weather data recorded over the experimental growth season (2014-2015).

Table 4.1 *Monthly meteorological variables measured during the 2014/2015 sugar beet growing season at a nearby standard weather station of the Agroclimatic Information Network of the Andalusia government. P (mm): rainfall; Tm (ºC): mean air temperature; RHm (%), mean relative humidity; u (m s-1), mean wind speed; Rs (MJ m-2 day-1), solar radiation; ET0 (mm day-1), mean FAO-Penman Monteith reference crop evapotranspiration.*

Date	P	T_m	RH_m	u	R_s	ET_0
	mm	°C	%	m s^{-1}	MJ m^{-2} day^{-1}	mm day^{-1}
Oct-14	66	20.5	71.3	2.1	15.0	3.4
Nov-14	185	15.4	82.2	2.7	9.8	1.9
Dec-14	49	9.9	87.9	2.3	8.7	1.2
Jan-15	151	9.7	85.4	2.9	10.3	1.5
Feb-15	17	10.9	77.9	3.3	13.2	2.2
Mar-15	50	13.1	79.1	2.3	17.4	3.0
Apr-15	35	16.3	76.3	3.2	21.5	4.1
May-15	7	20.7	59.8	2.6	27.2	6.2
Jun-15	9	22.4	60.4	2.5	26.8	6.2
Jul-15	9	24.7	69.0	1.8	28.7	6.3

4.2.2. Soil characteristics and variability

Soil variability was characterized by conducting two complementary tests. Soil texture was measured based on thirty soil samples collected at a depth of 300 mm using a soil auger. Soil analyses were performed in the Centre for Research, Technology and Innovation (CITIUS Laboratory) at the University of Seville. Systematic sampling was performed by maintaining a fixed distance between two sampling points (using a net or mesh). All samples were georeferenced using a differential-global navigation satellite system (DGNSS) receiver and geographic information system (FarmWorks, Trimble Navigation Ltd., Sunnyvale, CA, USA) distribution maps of different soil properties compiled using a kriging technique (Goovaerts, 1997).

Apparent electrical conductivity (ECa) was measured using an EMI Dualem-21S sensor (DUALEM, Milton, Canada) operated at a height of 75 mm above the soil surface and sheltered in a customized polyvinyl chloride case. The equipment was pulled by an all-terrain vehicle (Figure 4.1a) and was coupled to a real-time kinematic differential global positioning system (Trimble, Sunnyvale, CA) to collect samples over a 12 ha swath of the field site. Measurements were collected in parallel swaths from NE to SW separated by 10 m with the aid of a guidance system; points within a swath were separated by 1-2 m. We also collected samples along 23 NW to SE swaths to increase the sample density. The sensor was operated at a fixed frequency of 9 kHz and consisted of a transmitter coil at one end and four receiver coils that were separated from the transmitter coil by 1, 1.1, 2, and 2.1 m. The receiver coils were oriented in a perpendicular (PrP) or horizontal co-planar (HCP) configuration with respect to the transmitter coils. Each transmitter-receiver combination provided integrated ECa values for the corresponding explored soil volumes; these values depended on the exploration depth of each signal. The effective depth of exploration is the depth over which an array accumulates 70% of its total sensitivity, which also depends strongly on the ECa of the soil (Callegary et al., 2007). The theoretical exploration depths for the 1.1 and 2.1 m HCP and the 1 and 2 m PrP coil combinations were 0.5, 1.0 and 1.6 and 3.2 m, respectively. At high values of true conductivity, the sensor has a non-linear response, and ECa is increasingly underestimated for a given frequency and intercoil spacing

(McNeill, 1980). Beamish (2011) proposed a correction procedure involving a least-squares polynomial fitted to the theoretical deviation of the linear relationship between LIN-approximated ECa and the true conductivity of the coil configurations to allow for the correction of the LIN approximation breakdown. This approach was adopted in this study, and the corrected LIN-approximated ECa is used hereafter. The coefficients used for the polynomial fitting are available in Delefortrie et al. (2014). The final transformation applied to the raw ECa data accounted for the soil temperature effects. A reference temperature of 25°C is typically used (Corwin and Lesch, 2005):

$$\mathrm{ECa}_{25} = \mathrm{ECa}\left[0.447 + 1.4034\mathrm{e}^{-\left(\frac{\mathrm{T}}{26.815}\right)}\right] \quad (4.1)$$

where ECa25 is the standardized ECa at a temperature of 25°C, and T is the soil temperature in °C. To simplify the nomenclature, we use ECa as the temperature-corrected ECa (ECa25) reading. The average soil temperature at a depth of 0-0.30 m, obtained from 30 samples collected across the field, was used. Given the high correlations between signals observed in the field (correlation coefficients ranging from 0.9 to 0.94), we used the 1.1 HCP signal that best represented the rooting depth of the sugar beet crop. The FAO has established a range of maximum effective rooting depths for sugar beet, i.e., 0.7-1.2 m (Allen et al., 1998). The ECa data were filtered to remove spurious errors and were interpolated by means of ordinary block kriging on a 2 x 2 m grid to create maps for the four ECa signals using the geostatistical analyst in ArcGIS (ESRI, Redlands, CA) (Figure 4.1b). We used an anisotropic spherical model to fit the variogram with a lag size of 1.5 m, range of 75 m, sill of 1663 (mS m^{-1})^2 and 115° as its main direction. A cross validation of the interpolation yielded a root mean squared error of 6.5 mS m^{-1}.

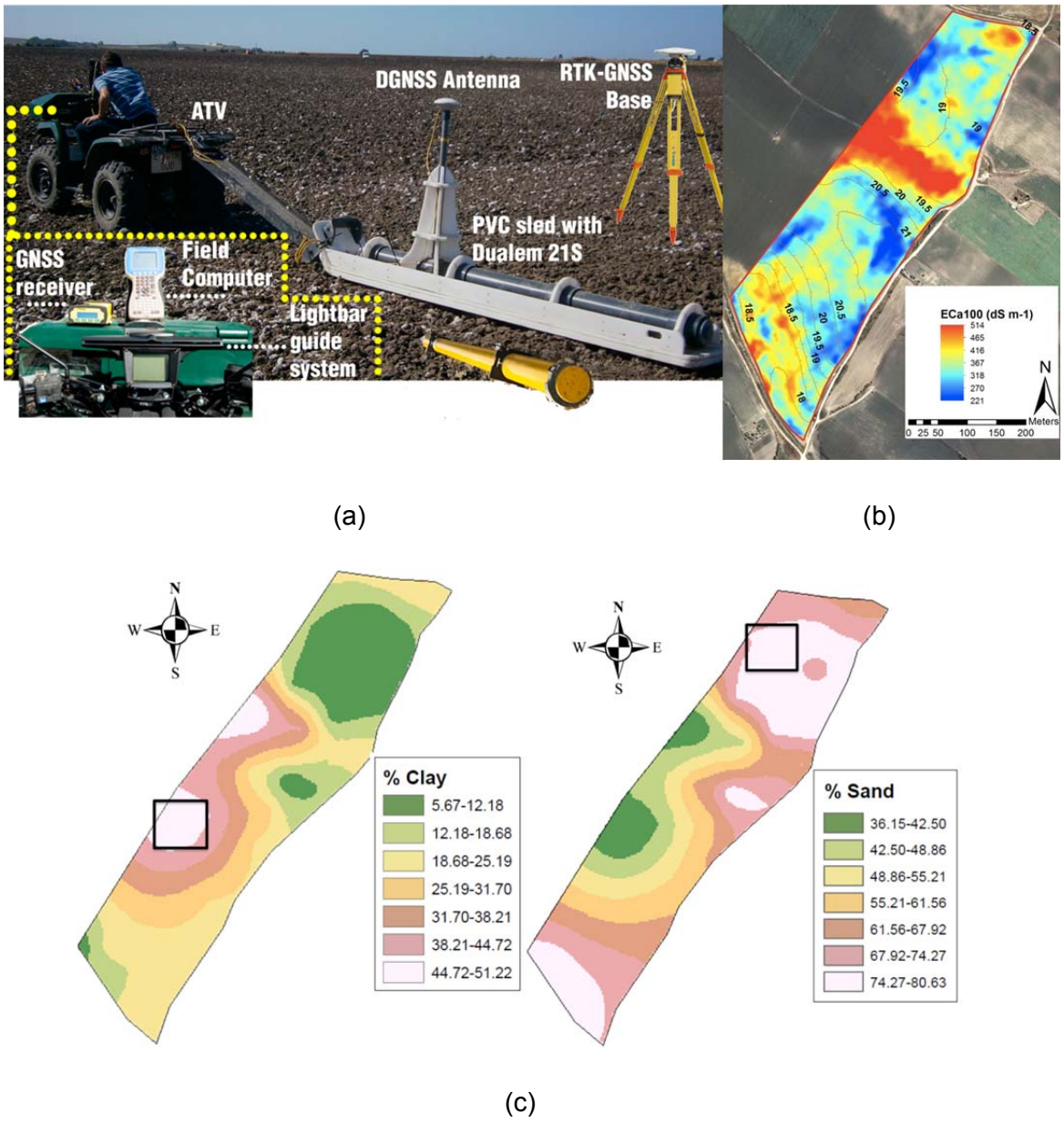

Figure 4.1 *a) Dualem sensor. b) CEa map obtained at a depth of 1000 mm. c) Clay and sand content maps. The squares indicate the selected zones.*

4.2.3. Mapping soil heterogeneity and selection of experimental plots

The soil texture maps generated using Farm Works (Trimble Navigation Ltd.) mapping software (Figure 4.1c) showed strong soil variability. Two zones of extremely high soil texture variability were identified; one with prevailing clayey soil, and the other with sandy soil (Figure 4.1c). Within each of the selected areas (clayey and sandy zones), two experimental plots (4 in total) covering an area of approximately 72 m^2 (i.e., the area within three adjacent sprinklers,

considering that a triangular arrangement of sprinklers was established) were established. The visual confirmation of the ECa maps (Figure 4.1b) with the soil texture maps confirmed that the selected clayey and sandy zones presented relatively uniform medium and low range ECa values, respectively.

4.2.4. Soil moisture measurements

Soil moisture was measured in the 0-1000-mm soil profile during the study period using a multi-sensor PR-2 profile probe (Delta-T Devices, Ltd., Cambridge, UK). Two epoxy-fibreglass access tubes with a rubber-sealing plug were buried in each experimental plot. The PR-2 is a polycarbonate rod with six pairs of stainless steel rings at 100, 200, 300, 400, 600 and 1000 mm, and soil moisture was measured at these depths. The PR-2 probe was calibrated for each soil zone (i.e., the selected clayey and sandy zones), and the manufacturer's equation (Qi and Helmers, 2010) was applied to convert the permittivity into volumetric soil water content. For the calibration, undisturbed soil samples were collected near the access tubes at the end of the growing cycle over several days to ensure a broad range of soil moisture conditions. Bulk density and volumetric moisture content were determined for each sample. The moisture measurements collected using the PR-2 probe and those obtained in the laboratory were used to determine the calibration curves for each soil type. Once calibrated, the soil moisture measurements in the 0-1000-mm soil profile were used to calculate changes in the relative extractable water (REW) for all experimental plots using the following expression:

$$\mathrm{REW} = \frac{\mathrm{R} - \mathrm{R_{min}}}{\mathrm{R_{max}} - \mathrm{R_{min}}} \quad (4.2)$$

where R is the soil moisture content, and R_{max} and R_{min} are the soil moisture contents at the field capacity and wilting point, respectively. R_{max} and R_{min} were determined using the Rosetta model, which is based on the van Genuchten model (Van Genuchten, 1980), and the soil physical properties measured in each selected zone (i.e., sand, clay and silt fraction; bulk density).

4.2.5. Thermal imaging and Unmanned aerial vehicle description

Thermal images of the sugar beet fields were acquired using an uncooled Tau 2 324 thermal camera (FLIR Systems, Inc., Oregon, USA). The main characteristics of the camera are summarized in Table 4.2. The accuracy of thermal measurements performed using this type of camera mounted on a UAV has been reported to be approximately 1K (Berni et al., 2009).

The camera was installed in a vertical orientation in the middle of the bottom of the UAV, which was a small Phantom 2 multi-rotor copter (SZ DJI Technology Co., Ltd., Shenzhen, China) equipped with a GNSS receiver. The UAV, which had a flight duration of 25 min and a remote control range of 1,000 m in open spaces, was controlled by the DJI iPad Ground Station application.

The UAV was flown across the experimental field on six clear-sky days over the period from day of year (DOY) 86 to DOY 167. The flights, which were performed at solar noon, measured surface temperature over the four experimental plots at several heights (5 m, 10 m, 20 m, 30 m and 40 m) above the ground level. The flight time over the different experimental plots and at several heights did not exceed 30-40 min in order to minimize the differences in weather conditions during the period of measurement. The thermal images were acquired at a rate of 9 frames per second and were stored on-board in a raw format with 14-bit radiometric resolution. A total number of 50 selected thermal images were analysed during the growth season.

Table 4.2 *Thermal camera technical data.*

Camera Features	
Scene range	-25 ˚C to 135 ˚C
Detector	Vanadium Oxide (VOx) microbolometer
FPA / video display format	324 x 256 pixels
Infrared lens	9 mm f/1.25
Temperature sensitivity	<50 mK
Wide field of view	48º x 37º
Full frame rates:	30/60 Hz
Pixel pitch	25 µm

The thermal images captured by the UAV were used to calculate the mean sugar beet temperature of each experimental plot by averaging the temperature of the pure vegetation pixels. Pure vegetation pixels were extracted from the thermal image using a segmentation algorithm written in R (R Core Team, 2015) and based on a histogram analysis of pixels from each thermal image (Figure 4.2) and the 'full width at half maximum' (FWHM) rule. The FWHM rule allows identification of pixels with high probability of being pure vegetation, as described elsewhere (Rud et al., 2015; Käthner et al., 2017). The assessment of crop water status was based on the difference between the average temperature of the vegetation cover and the prevailing air temperature at the time of flight (∆T), measured using the air temperature sensor (model HMP45C, Vaisala, Helsinki, Finland) installed at the nearby weather station (absolute precision of ±0.2ºC). Values of ∆T were also used to determine a cumulative integral of the degree of crop water stress throughout the irrigation season. The difference between ∆T and the corresponding value for a non-stressed canopy provides the difference in canopy temperature, or degree of stress, for a specific sampling date. This indicator, DANS, was adapted by DeJonge et al. (2015) to integrate the impact of water stress throughout a whole day. In this study, an expression analogous to the water stress integral (WSI), originally proposed by Myers (1988) for predawn leaf water potential measurements, was used to determine the cumulative integral of water stress over the entire irrigation season as measured by differences in canopy temperature:

$$\mathrm{WSI}\ (°\mathrm{C\ day}) = \sum_{i=0}^{i=t}\left(\Delta T_{i,i+1} - c_{i,i+1}\right)n \qquad (4.3)$$

where t represents the number of ΔT measurements (t=6), in agreement with the number of flights conducted); ΔTi,i+1 is the average ΔT for any interval i, i + 1; ci,i+1 is the average of the non-water-stressed ΔT values for any period i, i + 1; and n is the number of days in the interval. The c values were obtained from the non-water-stressed baseline (NWSB) derived by Idso (1982) to calculate the CWSI for sugar beet:

$$c_i = a + bVPD_i \qquad (4.4)$$

where VPDi represents the prevailing vapour pressure deficit (kPa) at the time of flight on the ith measurement day, and a and b are two parameters

obtained empirically for each species under specific environmental conditions. The a and b values for sugar beet on sunny days are a 2.50 and -1.92, respectively (Idso, 1982). The VPD and air temperature data at a height of 2 m were obtained from a nearby weather station belonging to the Agroclimatic Information Network of the Andalusia government.

The Idso (1982) NWSB was also used to calculate the CWSI of the ith sampling day as follows:

$$CWSI = \frac{\Delta T_i - c_i}{\Delta T_{dry,i} - c_i} \quad (4.5)$$

where ΔTdry,i represents the maximum ΔT, which corresponds to a non-transpiring canopy. In this case study, it was found that the sugar beet leaf temperature could reach up to 8ºC above air temperature; consequently, a constant ΔTdry,i = 8ºC was considered. Similar ΔTdry,i values have been found for other herbaceous crop species (Rud et al., 2014).

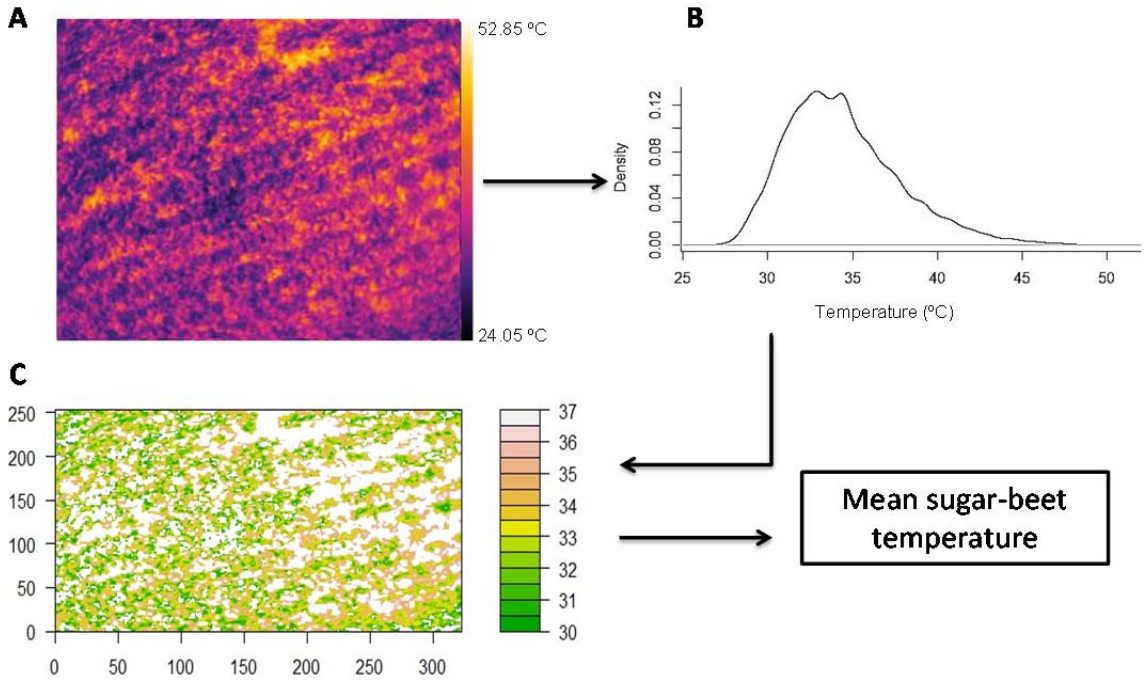

Figure 4.2 *Thermal image processing performed in this field trial to derive the mean sugar beet temperature in each experimental plot. The segmentation algorithm is based on a histogram analysis and the FWHM rule. (A) Thermal image of a sugar beet field plot; (B) distribution of temperature in the thermal image depicted as a density histogram; (C) segmented thermal image in which the regions of interest have been selected.*

4.2.6. Irrigation strategy

Two experimental plots were established in each of the selected soil zones, i.e., the clayey and sandy areas of the experiment. In each soil zone, one of the plots was irrigated following the criteria used by local farmers (WW to indicate presumably well-watered conditions), and in the other experimental plot, two water stress cycles were imposed by withholding irrigation through nozzle blinding of adjacent sprinklers for approximately three weeks per cycle (WS to indicate water-stressed conditions). A recovery period of 24 days was established between both water deficit cycles. The irrigation depths applied to the WW and WS plots over the entire growing season were 320 mm and 170 mm, respectively. The irrigation depth applied during each irrigation event was 30 mm, except one where 20 mm was applied. Irrigation frequencies were determined from the cumulative crop water requirements calculated following the FAO-Penman-Monteith method (Allen et al., 1998).

4.2.7. Production

Sugar beet yield was evaluated in the four experimental plots by manual harvesting six samples per experimental plot at the end of the growing season (early July). Fresh root mass (t ha^{-1}), sugar recovery (%) and sugar content (t ha^{-1}) were determined for each sample.

4.2.8. Statistical analyses

Analysis of variance (ANOVA) performed with the statistical package Statgraphics (Statgraphics Centurion XV) was used to compare the yield components and yield between treatments. The relationships between yield, components and the water stress integral were evaluated using linear regression analysis in Statgraphics software.

4.3. Results

4.3.1. Soil moisture

The soil moisture dynamics of the four selected plots are shown in Figure 4.3. The WW_{Sand} plot maintained REW values close to one (field capacity)

throughout the study period. However, the WW_{Clay} plot could not maintain field capacity conditions throughout the irrigation season, and REW decreased to approximately 0.6 during the period from DOY 80 to 125 even though the irrigation scheduling in both the WW_{Clay} and WW_{Sand} plots was similar.

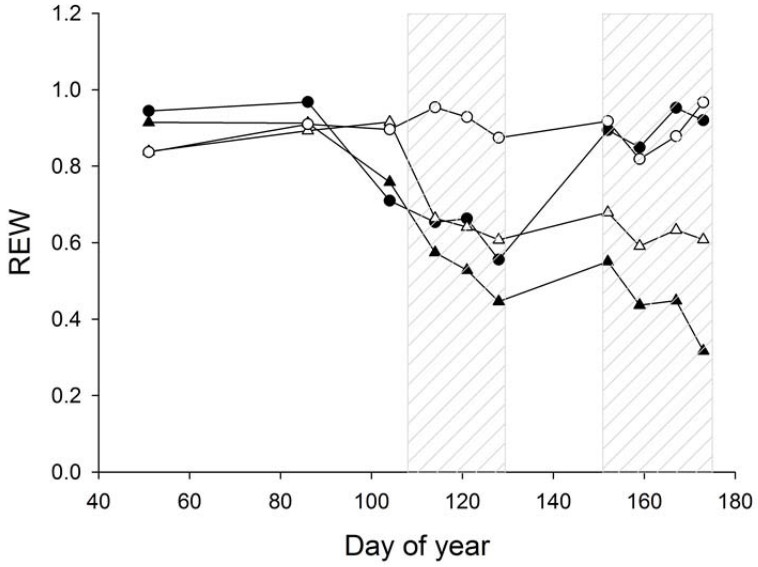

Figure 4.3 *Seasonal time courses of the relative extractable water fraction (REW) in the 0-1000-mm soil profile of the four study plots. Each point represents the average of two measurements per plot. The hatched areas indicate the periods during which irrigation was withheld in the WS_{Clay} and WS_{Sand} plots. Definition of symbols: filled triangles (WS_{Clay}), hollow triangles (WS_{Sand}), filled circles (WW_{Clay}), hollow circles (WW_{Sand}).*

The REW dynamics in the WS_{Sand} and WS_{Clay} plots were similar throughout the study period, although WS_{Clay} exhibited REW values that were consistently 15-20% lower than those observed in WS_{Sand} (Figure 4.3). The restitution of irrigation after the first water deficit cycle in the WS treatments did not allow soil moisture values to reach those of the WW treatments in any of the study plots.

4.3.2. Crop temperature

The crop temperatures determined from thermal imaging for all experimental plots at various flight altitudes and on six sampling dates during the irrigation season were averaged for each flight altitude to analyse the effect of height (from 5 to 40 m) on the estimated crop temperature. The mean crop temperatures of the four experimental plots averaged across the six flight dates were similar ($P>0.05$) within the 5-40-m height range (Figure 4.4).

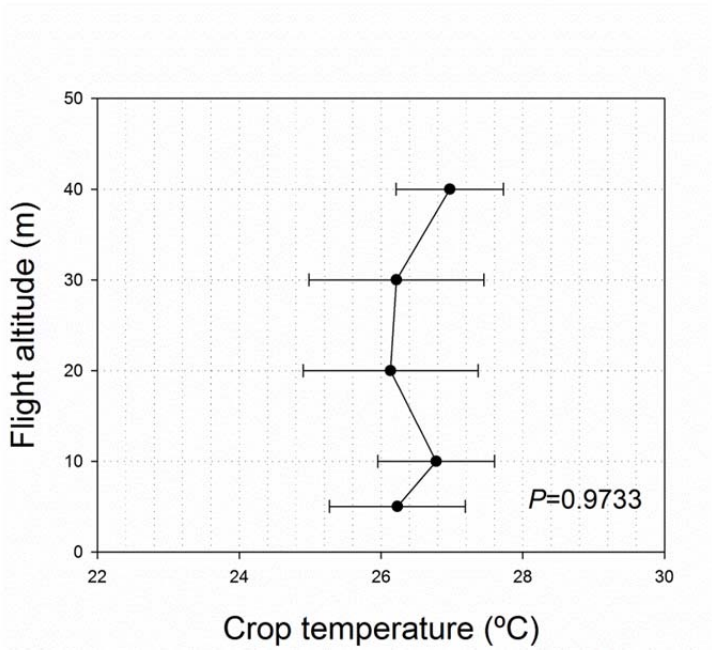

Figure 4.4 *Crop temperatures determined at flight altitudes from 5 to 40 m. Each point represents the six-flight average of mean crop temperature determined for the four experimental plots. The error bars indicate the standard error of the mean.*

The mean crop temperatures at 30 m were used to calculate the crop-air temperature differences (ΔT) and CWSI for each experimental plot throughout the study period (Figure 4.5). A comparison of the ΔT dynamics derived for WW_{Clay} and WW_{Sand} showed that WW_{Sand} had lower ΔT values than WW_{Clay} at the beginning of the trial (DOY 85-115) and higher ΔT values from DOY 130 onwards (Figure 4.5a). In the plots with irrigation deficits (WS), WS_{Sand} had lower ΔT values than those of WS_{Clay} at the beginning of the trial (DOY 85-115), but ΔT was consistently higher in WS_{Sand} than in WS_{Clay} from DOY 115 onwards (Figure 4.5b). A comparison of the WW and WS plots for each soil type revealed that in the clay soil, ΔT was only slightly affected by the soil moisture differences (Figure 4.3) caused by irrigation management. However, in the sandy soil, the ΔT of WS_{Sand} was substantially higher than that of WW_{Sand} from approximately DOY 115 (onset of the first water-stress cycle; Figure 4.3). Similar seasonal trends to those described for ΔT were also observed for the CWSI (Figures 4.5c, 4.5d). The CWSI values ranged fron 0 to 1 across most of the experimental plots and sampling dates, but negative values observed in the sandy plots on one of the sampling days suggest that the Idso (1982) NWSB

may not be suitable for the prevailing environmental conditions of this study area.

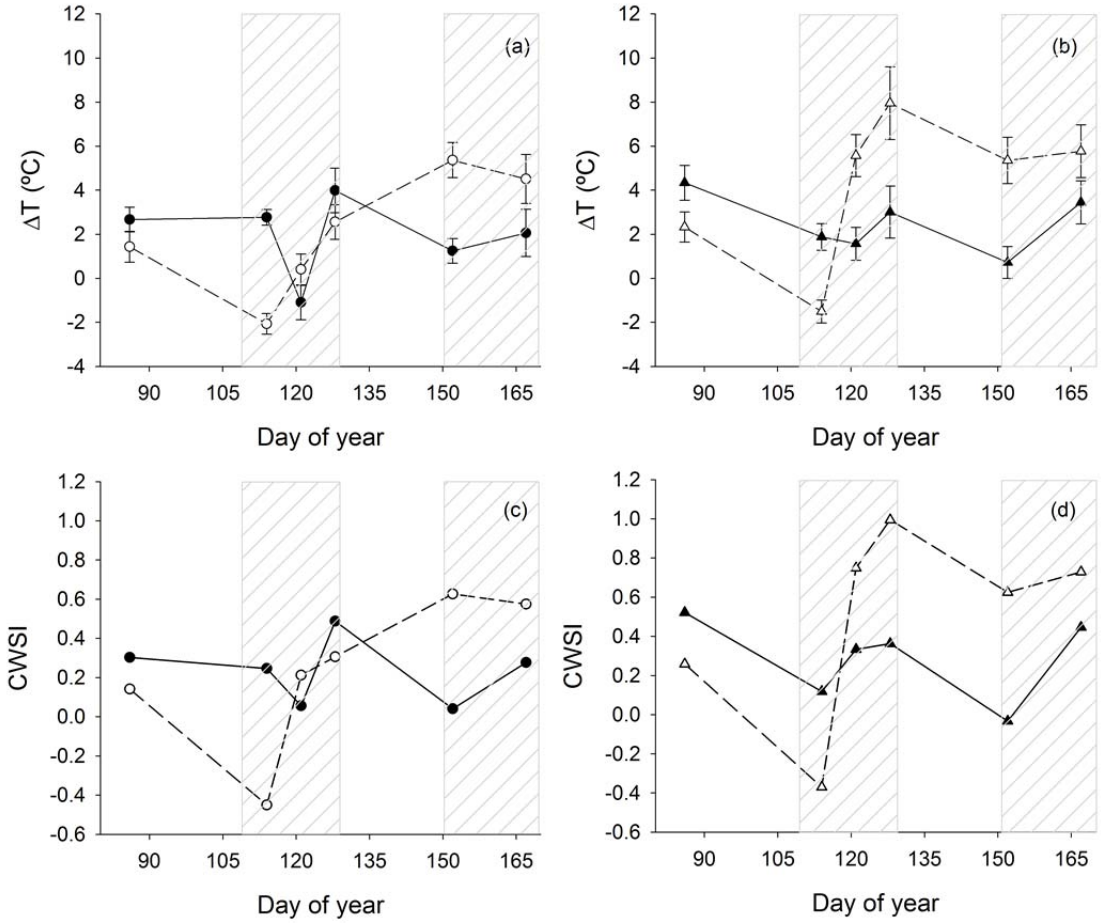

Figure 4.5 *Evolution of the crop-air temperature difference (∆T) and crop water stress index (CWSI) in WW_{Clay} and WW_{Sand} (a, c) and WS_{Clay} and WS_{Sand} (b, d) plots The crop temperature was measured at a flight altitude of 30 m. Error bars indicate the standard error of the mean. The hatched areas indicate the periods during which irrigation was withheld in the WS_{Clay} and WS_{Sand} sub-plots. Definition of symbols: filled triangles (WS_{Clay}), hollow triangles (WS_{Sand}), filled circles (WW_{Clay}), hollow circles (WW_{Sand}).*

Table 4.3 shows the sugar beet yield components determined at harvest for all experimental plots. Irrigation management had a significant effect on sugar beet yield in both soil types, although a more negative impact of water stress was observed in the sandy soil. In the clay soil, WS_{Clay} showed a significant decrease in fresh root mass compared to WW_{Clay}, but this reduction was not translated into a sugar content reduction since the sugar recovery rate of WS_{Clay} was significantly higher than that of WW_{Clay}. In the sandy soil, both the fresh

root mass and sugar content were significantly lower in WS_{Sand} than in WW_{Sand}, while no differences in sugar recovery rate were observed in this soil type. The soil type had also a significant impact on sugar beet fresh root mass, as indicated by the lower values observed in both WW_{Clay} and WS_{Clay} than in the corresponding sandy plots. The soil type had no effect on the sugar content, as similar sugar contents were measured in WW_{Clay} and WW_{Sand} as well as in WS_{Clay} and WS_{Sand}.

Table 4.3 *Sugar beet yield components measured in the experimental plots.*

Plot ID	Fresh root mass	Sugar recovery	Sugar content
	(t ha^{-1})	(%)	(t ha^{-1})
WW_{Clay}	104.0 ± 3.7b	14.8 ± 0.2b	15.4 ± 0.6a
WS_{Clay}	83.0 ± 1.5d	17.9 ± 0.3a	14.8 ± 0.3ab
WW_{Sand}	115.5 ± 4.3a	14.2 ± 0.1b	16.3 ± 0.6a
WS_{Sand}	93.2 ± 1.5c	14.6 ± 0.4b	13.6 ± 0.2b

Different letters within the same column denote significant differences based on Duncan's multiple range test.

In an attempt to integrate the cumulative water stress in the experimental plots during the measurement period, a WSI was calculated for all plots based on the ΔT measurements and an adaptation of the expression originally developed by Myers (1988) to quantify the cumulative integral of leaf water potential over any chosen period of time. The derived WSI was related to sugar beet yield (both fresh root mass and sugar content), as shown in Figure 4.6. The fresh root mass and sugar content tended to decrease linearly with increasing WSI. However, while the relationship between the fresh root mass and WSI was poor (R^2= 0.28), the WSI and sugar content were closely related, as shown by the high coefficient of determination of the linear regression (R^2= 0.94).

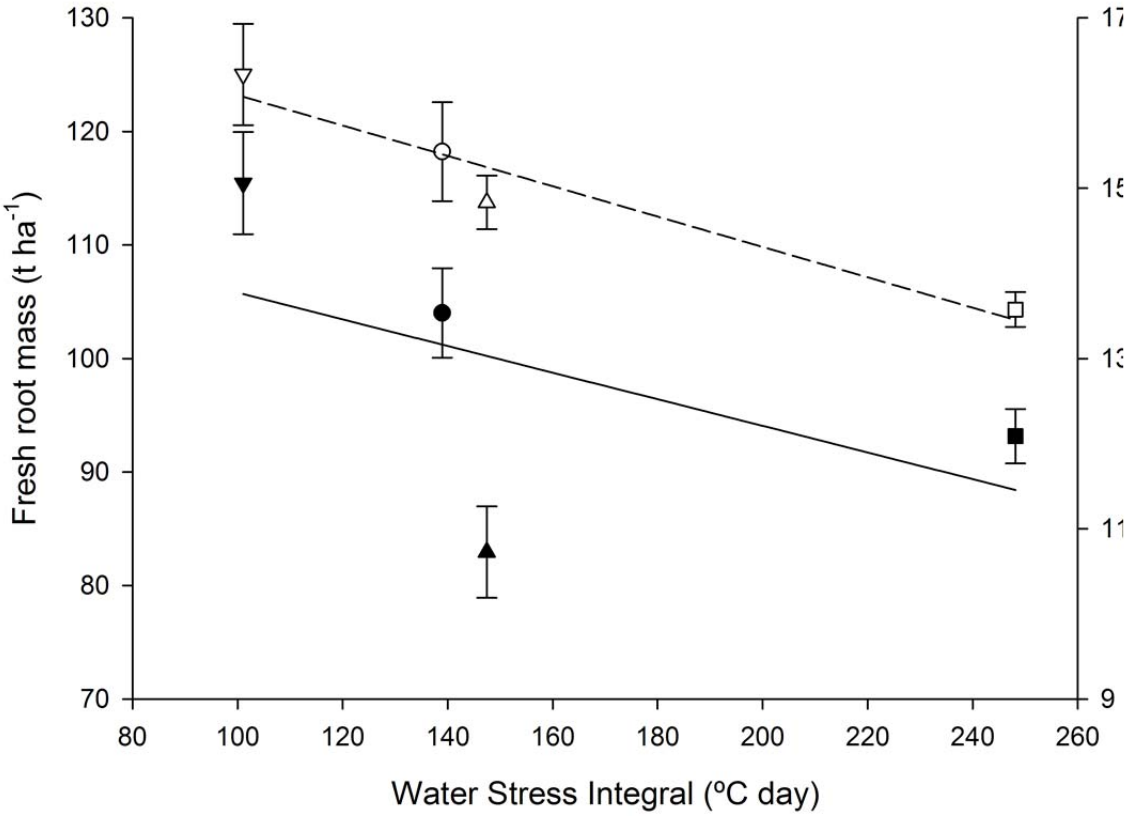

Figure 4.6 *Relationships of the fresh root mass (filled symbols) and sugar content (hollow symbols) with the water stress integral (WSI) determined from the cumulative crop-air temperature difference. Dashed line: regression line between the sugar content and WSI (y=17.8-0.018x, R^2=0.94). Continuous line: regression line between the fresh root mass and WSI (y=117.5-0.117x, R^2=0.28). Definition of symbols: hollow symbols (sugar content), filled symbols (fresh root mass); triangles pointed upward (WS_{Clay}), inverted triangles (WW_{Sand}), circles (WW_{Clay}), squares (WS_{Sand}).*

4.4. Discussion

This study provides further evidence of the impact that soil variability may have on crop performance when it is not considered as an additional factor of the production system. A uniform water supply in a non-uniform sugar beet field with strong soil texture variability led to differences in the REW between the clayey and sandy zones that were irrigated to satisfy crop water requirements (WW_{Clay} and WW_{Sand}, respectively) (Figure 4.3). The marked decrease in REW observed from DOY 80 to 125 in WW_{Clay} compared to that in WW_{Sand} (Figure 4.3) indicates the importance of considering soil variability in irrigation supply

decisions. Although clayey soils may retain more water than sandy soils, the soil moisture measured taken in the 0-1000 mm soil profile suggested that the plants grown in the WW_{Clay} plot extracted more soil water than those grown in the WW_{Sand} plot from DOY 80 to 125. Although crop growth measurements were not performed to support this hypothesis, the fraction of green vegetation or canopy cover (i.e., the fraction of ground covered by green vegetation) estimated on DOY 86 for both WW plots from the thermal images captured using the micro-UAV (Figure 4.7) revealed that the plants grown in the WW_{Clay} plot had 10% more canopy cover than the plants grown in the WW_{Sand} plot (see the caption of Fig. 4.7 for details on how plant cover was estimated). The faster canopy development observed in the WW_{Clay} plants can therefore explain the higher root water uptake observed in these plants compared with the WW_{Sand} plants.

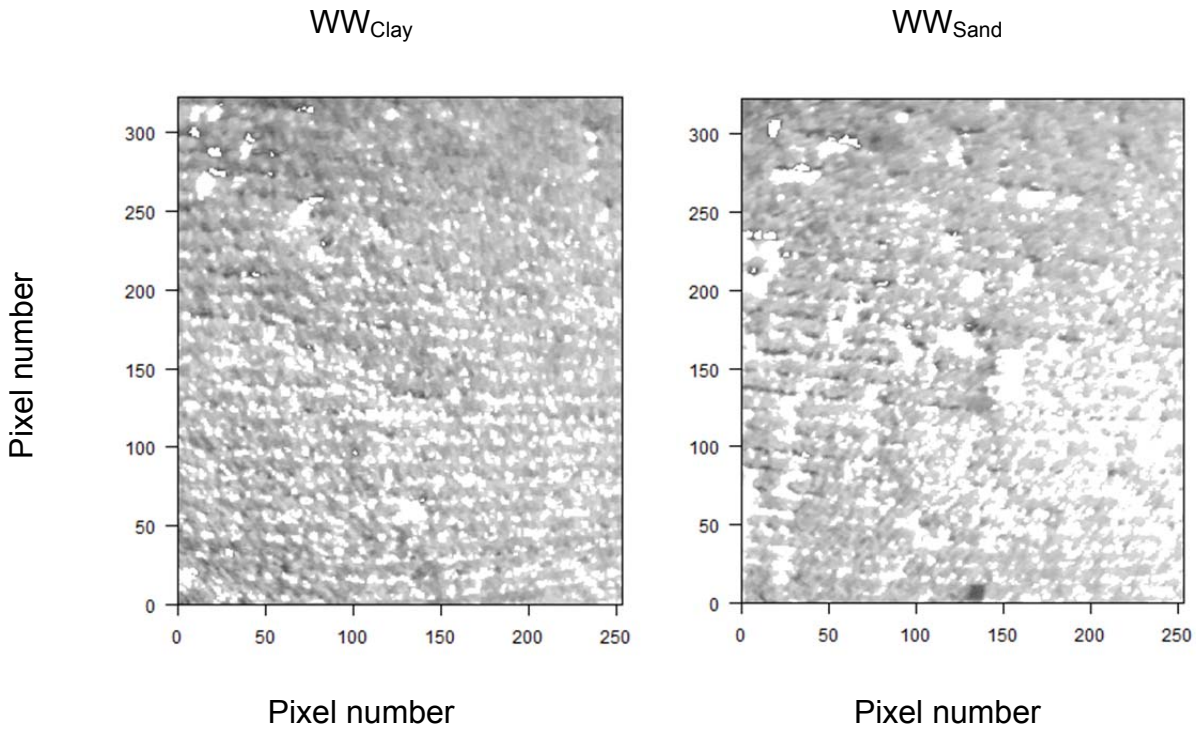

Figure 4.7 *Thermal infrared images of the WW_{Clay} (left) and WW_{Sand} (right) plots with marked segments distinguishing between the background (soil) and regions of interest (vegetation). A segmentation algorithm based on the FWHM rule was applied. The IR thermal images were captured at a flight altitude of 20 m on day of year 86. Estimates of canopy cover were 90.77% and 80.96% in the WW_{Clay} and WW_{Sand} plots, respectively. WW indicates well-watered conditions.*

Despite the valuable information provided by soil moisture sensors to support irrigation decisions, drawbacks of this technique in terms of acquiring accurate and representative soil moisture information have also been reported (Jones, 2004). The derivation of crop water stress indices from aerial thermal images represents a promising decision support tool to complement soil moisture information in irrigation programmes (Bellvert et al., 2014). The results obtained in this study suggest that during some periods of the sugar beet irrigation season, the soil moisture content determined from two probes per plot could not reproduce the dynamics of the derived thermal index, a surrogate of crop transpiration. This was the case for the plants grown in the WS_{Sand} plots, which had higher REW values than the WS_{Clay} plants (Figure 4.3). Moreover, the ΔT and CWSI values, which are used as proxies for the mean crop water stress (Maes and Steppe, 2012), were also higher in the WS_{Sand} than in the WS_{Clay} plots (Figure 4.5) over the two cycles of imposed water stress. Furthermore, the WW_{Clay} and WW_{Sand} plots had similar REW values from DOY 150 onwards, while the corresponding mean ΔT and CWSI values were higher in the WW_{Sand} plants than in the WW_{Clay} plants. These findings highlight the differences in crop transpiration between the WW plots and suggest that soil moisture data measrued in a small number of locations may not be reliable enough to represent the mean crop water status of zones with uniform soil properties. Poor relationships between canopy temperature-based indices and soil moisture deficits are frequently observed (DeJonge et al., 2015) and drive which is fostering the search for remote sensing applications that use the crop as an intermediate sensor for quantifying soil water availability (Zhang et al., 2011).

Thermal indices derived from satellites and airborne observation platforms flying at high altitudes require complex post-processing to correct of parameters such as atmospheric transmissivity (Berni et al., 2009), which decreases with relative humidity, temperature and distance from the object (Sugiura et al., 2007). In arid and semi-arid regions, relatively stable atmospheric conditions prevail when thermal measurements are conducted at the same time of during the day under clear-sky conditions and during the months of high evaporative demand (irrigation season). This implies that thermal errors caused by variations in atmospheric transmissivity during low-altitude flights may be

related to camera error. We assessed this possibility and found no significant differences in the mean crop temperature at flight altitudes of 0-40 m (P=0.9773) (Figure 4.4).

WSI values calculated from other non-thermal plant-based water stress indicators (e.g., predawn leaf water potential or stem water potential) and for different crop species showed great potential to predict yield losses due to water stress (Ginestar and Castel, 1996; Egea et al., 2013). The close relationship observed between sugar production and the temperature-based WSI (Figure 4.6) indicates that T-based WSI was sensitive enough to capture the impacts of both soil heterogeneity and irrigation management on sugar production, thereby confirming the reliability of the method described in this work for monitoring the cumulative water stress in sugar beet fields.

From an irrigation scheduling perspective, use of the CWSI as a crop water stress indicator for sugar beet requires further experimentation. Although this index is a sensitive indicator that is able to capture the differences between plants grown in sandy or clay soils and between well-watered plants and those subjected to intentional water shortages, aspects such as the derivation of a wet reference baseline adapted to Mediterranean conditions and local cultivars and the definition of threshold values for irrigation management based on relationships with other plant physiological variables (e.g., leaf gas exchange variables) need to be determined.

4.5. Conclusions

The results of this study yielded two clear conclusions. First, the canopy-air temperature differences and the CWSI values determined from thermal images captured using a micro-UAV were sensitive enough to identify variations in crop water use resulting from different irrigation management strategies or the natural variability of soil properties. Second, the dynamics of the soil moisture content determined from a limited number of sampling points (two probes per plot in this study) failed to adequately represent the variation in crop water use, as estimated from the thermal indices derived. This study presents a reliable method to monitor the spatio-temporal variations of crop water use in sugar beet fields, although further research is required to transform this information

into optimal recommendations for sugar beet irrigation requirements. A temperature-based WSI was demonstrated to be a good predictor the sugar content at harvest under both soil variability and irrigation management.

Acknowledgments

Financial support provided by the Spanish ministry of Economy and Competitiveness (Research Project AGL2013-46343-R) and the Regional Government of Andalusia (Research Project P12-AGR-1227) is greatly appreciated.

Chapter 5: Main results and general discussion

This chapter presents the main results obtained in this Doctoral Thesis as well as their implications for the agricultural sector. Until the 1980s, agriculture did not pay any attention, at least in a systematic way, to the spatial variation in soil and/or crop properties. The division of heterogeneous fields into management units that can be considered homogeneous has been, conceptually, a great advance for agriculture since it allows more efficient management of inputs, improved yields and/or crop quality and increased environmental sustainability. However, due to the number of technologies involved, the concept of precision farming has spread out faster than the development of applications commercially and affordably available for farmers.

This thesis has contributed to narrowing the gap that still exists between the concept of precision agriculture and its application in the field. In particular, it has led to the development of two approaches for accurate nitrogen application in one of the most economically important rain-fed crops in Andalusia (wheat) and irrigation in one of the most economically important irrigated crops in Western Andalusia (sugar beet).The implementation of precision agriculture implies the use of tools and technologies with different levels of development, independent of each other but totally linked from the point of view of achieving the final objective. The different levels of technologies that can be used in precision farming applications, such as the ones developed in this Thesis, are grouped below:

- Global Navigation Satellite Systems (GNSS): systems that provide agricultural equipments/sensors positioning with various levels of accuracy.
- Soil and crop sensing devices: proximal and remote sensors that retrieve information from soil and plant tissues in a more timely and less costly way than collecting samples to be analyzed in the laboratory.
- Geographic Information Systems (GIS): tools for georeferenced management and mapping of parcel information (e.g. yield and other agronomic parameters to be cross-correlated for developing next season’s management strategies).

- Variable Rate Technology: electronic and positioning technologies on board field machinery capable of fulfilling the variable rate of crop requirements.

In order to carry out variable rate application of any type of crop input, such as fertilizers or irrigation water, it is of utmost importance to develop, as a first step, methodologies to characterize the spatial-temporal variability of relevant soil/crop traits.

That has been the sense of this Thesis, whose objectives have been focused on developing methodologies to determine the spatial-temporal variability of N- and water status- related crop traits for variable rate fertilizer and irrigation application in wheat (Chapter 3) and sugar beet (Chapter 4), respectively.

Spatial variability of wheat traits for variable-rate nitrogen fertilizing (Manuscript 1)

In Andalusia, due to the structure of agricultural fields devoted to arable crops (small to medium sized fields), yield monitoring is already been considered by some farmers as the main entry-level technology for use in precision agriculture. In this region, wheat fields accounts for 33% of the area under arable crops (around one million hectares), which suggests the economic and environmental importance of this crop in the region. Within a particular farm, the spatial differences in wheat yields are reflecting differences in soil conditions that could be corrected, for example, by site-specific fertilizing. These conditions are structural and are often reflected in the same patterns in the yields of each year.

In this sense, the aim of this work was to analyze the extent to which the yield differences observed in a commercial winter wheat field are explained by means of an affordable proximal NDVI sensor, as well as the extent to which this indicator is related to differences in foliar nitrogen content.

The results obtained show that, in the two plots evaluated, NDVI and wheat yield were highly correlated, as shown by Pearson's correlation coefficients of 0.64 and 0.78 in plots 1 and 2, respectively. This high level of correlation is also evident when yield and NDVI maps are visually compared. This implies that

NDVI measurements can be used to delimit management zones in winter wheat grown under the prevailing conditions of Andalusia.

The strong linear correlation found between the percentage of foliar N content and NDVI measurements (with Pearson's correlation coefficients of 0.71-0.89) further suggests that the spatial variability of NDVI, and thus yield, are caused by variations in leaf N content across the fields. This finding has major implications for correcting yield heterogeneity or, at least, optimizing N-based fertilization for current site-specific needs.

In this regard, a possible application of the affordable NDVI sensor used in this work is to perform variable rate N management for winter wheat. In the same campaign and field, a further test evaluated the relationship between NDVI and the rates of total N applied (55, 150, 190, 225 and 250 kg ha^{-1}). The relationship among both variables was clearly exponential with a regression coefficient (R^2) of 0.99.

The use of optical sensors resulted in NDVI measurements that ranged between 0.60 and 0.78 in both fields. This information, along with the standard spatial interpolation method of IDW (Inverse Distance Weighting), allowed for variable-rate N prescription maps to be generated on an appropriate grid (12 m × 12 m) using field positions taken from a GNSS receiver.

Based on the prescription maps obtained, two theoretical farmer scenarios were created for variable-rate N application, conservative and risk taking, based on the number of N units to be distributed in the field.

The conservative scenario would be the one to be applied when the customary N units that are used in the area (not less than those that are usually placed) are distributed in such a way that more N-units are applied in areas where higher yields are expected and less N units are applied in areas with lower margin to increase yield. In terms of fertilizing cost, this scenario would not lead to significant savings.

However, in the most risky scenario, the intention would be to reduce the amount of N units applied in the field by applying the customary N units recommended in the area (240 kg N ha^{-1} in our case study) to the zones with

the greatest yield potential and reduce the amount in those zones with lower yield potential. This strategy would be the preferred option, for example, in cases in which the soil is a limiting factor to achieving higher yields irrespective of whether higher N rates are applied.

In the fields evaluated in this work, the risk strategy, in the case of being the most appropriate one, would have reduced the fertilizing cost by approximately 20%.

Spatial-temporal variability in sugar beet water status for precise irrigation management (Manuscript 2)

The goal of this study was to evaluate the use of thermal images captured using a micro-UAV to predict variations in sugar beet water status due to soil variability and irrigation management. For this aim, a commercial sugar beet field of about 12 ha and irrigated with a sprinkler system was used. In order to determine the impact that soil spatial variability has on sugar beet crop status, soil spatial variability was first characterized by measuring apparent electrical conductivity (ECa) with a EMI Dualem-21S sensor (DUALEM, Milton, Canada). With this information, two zones were selected to conduct the experiments, a clayey zone and a sandy zone.

In each soil zone, two plots were established, one irrigated following the criteria of the local farmers (WW, to indicate supposed good irrigation conditions) and the other plot submitted to water stress conditions (WS)

Soil moisture measurements performed with a PR2 profile probe (Delta-T Devices, Ltd., Cambridge, UK) at each selected plot confirmed that a uniform water supply in a non-uniform sugar beet field with strong soil texture variability leads to differences in soil water storage and crop development.

The poor spatial resolution of soil water measurements together with the difficulty to select appropriate sites for probes installation has motivated the need to derive methodologies to determine crop water status at higher spatial resolutions than those obtained with soil moisture monitoring. In this regard, crop water stress indices derived from aerial thermal imaging are showing

promising results to be used in decision support systems for irrigation management of various crops.

The results obtained in this study evidenced the difficulty that soil moisture content measured at a small number of sampling points has to represent the average crop water status of a homogeneous area. Thermal indices derived from crop temperature measured with a thermal camera on board a small sized UAV showed that (i) spatial variability in soil texture drives variations in sugar beet water status when irrigation is applied uniformly across the field, and that (ii) the impact of irrigation shortages on crop water status is also affected by soil type. In this regard, a comparison of the WW and WS plots for each soil type revealed that thermal indices were only slightly affected by deficit irrigation in clay soil, whereas the impact in sandy soil was substantially higher.

An important finding of this research, and that confirm the goodness of the thermal indices to characterize the sugar beet water status, is the close relationship found (R^2=0.94) between a thermal-based water stress integral (WSI) and sugar yield. The derived WSI was linearly related to sugar yield, such that the higher the WSI the lower the sugar yield, as also found for other non-thermal based WSI.

The close relationship observed between temperature-based WSI and sugar production indicates that this cumulative water stress index is sensitive enough to capture the impact of soil heterogeneity and irrigation management on sugar production.

From an irrigation scheduling perspective, the use of CWSI as water stress indicator still requires further experimentation. Although CWSI is sensitive and captures differences in crop water status between plants grown in sandy or clay soils and plants that are well irrigated or subject to deliberated water stress, aspects such as derivation of a wet baseline adapted to local conditions, or the definition of threshold CWSI values for irrigation management (based on their relationships with other physiological and agronomic variables) still need to be determined.

Chapter 6: Conclusions

This thesis analysed spatial variability in cereal and sugar beet fields by means of sensors and technologies commonly used in precision agriculture. In the first contribution, sensors' information was used to delineate differentiated management zones within the experimental plots for variable rate fertilization (Paper 1). In the second contribution, sensors' and instruments information was used to delineate management zones and assess crop water status for irrigation management (Paper 2). Main contributions with these two articles have been the following:

6.1 Spatial variability assessment in winter wheat for fertilization (Paper 1)

This research is looking for new and improved tools to help make decisions about the right amount of nitrogen fertilizer to apply to winter wheat fields in a particular year in a Mediterranean environment. The adoption of VRA nitrogen management has potential economic and environmental benefits. The main contributions are as follows:

- The average error of yield monitoring for detecting the actual mass flow rate was −3.1%, with a standard deviation of 4.2%. This monitoring enabled an assessment of the relationship between the yield data and NDVI measurements (r^2 = 0.64 and 0.78) for fields 1 and 2, respectively.
- The relationship between leaf N content and NDVI measurements from optical sensors (Greenseeker handheld sensor) gives determination coefficients greater than 0.9 in winter wheat.
- An appropriate and inexpensive portable hand-held optical sensor (GreenSeeker®, Trimble Navigation Ltd., Sunnyvale, CA, USA) could satisfactorily help operators predict and generate a map of N application recommendations for fields. Wheat canopy greenness may not always be the result of a certain N content (e.g., available water or temperature may also affect the greenness). If the greenness is not related to the N content, then N inputs are based on an erroneous indicator.
- N recommendation maps were developed, and accurate N recommendations for sub-regions of fields were produced. The

recommended N maps based on this technique may help operators use accurate and efficient application rates from year to year.

6.2 Spatial-temporal variability assessment in sugar beet fields for irrigation management. (Paper 2)

The results of this research yielded two clear conclusions:

- The canopy-air temperature differences and the CWSI values determined from thermal images captured using a micro-UAV were sensitive enough to identify variations in crop water use resulting from different irrigation management strategies or the natural variability of soil properties.
- The dynamics of the soil moisture content determined from a limited number of sampling points (two probes per plot in this study) failed to adequately represent the variation in crop water use, as estimated from the thermal indices derived.

This study presents a reliable method to monitor the spatio-temporal variations of crop water use in sugar beet fields, although further research is required to transform this information into optimal recommendations for sugar beet irrigation requirements.

A temperature-based WSI was demonstrated to be a good predictor of the sugar content at harvest under both soil and irrigation management variability.

REFERENCES

Allen, R.G., Pereira, L.S., Raes, D. and Smith, M. (1998). Crop evapotranspiration — guidelines for computing crop water requirements. FAO Irrigation and drainage paper 56. Rome: Food and Agriculture Organization

Arnó, J., Rosell, J.R., Blanco, R., Ramos, M.C. & Martínez-Casasnovas, J.A. (2012). Spatial variability in grape yield and quality influenced by soil and crop nutrition characteristics. *Precision Agric*ulture*, 13*, 393-410

Ballesteros, R., Ortega, J.F., Hernández, D. and Moreno, M.A. (2014). Applications of georeferenced high-resolution images obtained with unmanned aerial vehicles. Part I: Description of images acquisition and processing. *Precision Agriculture, 15*, 579–592

Beamish, D. (2011). Low induction number, ground conductivity meters: A correction procedure in the absence of magnetic effects. *Journal of Applied Geophysics*, *75(2)*, 244–253

Bellvert, J., Zarco-Tejada, P.J., Girona, J. and Fereres, E. (2014). Mapping crop water stress index in a “Pinot-noir” vineyard: Comparing ground measurements with thermal remote sensing imagery from an unmanned aerial vehicle. *Precision Agriculture, 15*, 361–376

Bellvert, J., Zarco-Tejada, P.J., Marsal, J., Girona, J., González-Dugo, V., and Fereres, E. (2016) Vineyard irrigation scheduling based on airborne thermal imagery and water potential thresholds. *Australian Journal of Grape and Wine Research, 22*, 307–315

Berni, J.A.J., Zarco-Tejada, P.J., Suárez, L. and Fereres, E. (2009). Thermal and narrowband multispectral remote sensing for vegetation monitoring from an unmanned aerial vehicle. *IEEE Transactions on Geoscience and Remote Sensing*, *47*, 722-738

Blackmore, S., Godwin, R., and Fountas, S. (2003). The analysis of spatial and temporal trends in yield map data over six years. *Biosystems Engineering*, *84(4)*, 455-466

Borgelt, S.C. (1993). Sensing and measurement technologies for site specific management. In *Soil specific crop management* (pp. 141–157). Madison, WI: American Society of Agronomy, Inc.

Bramley, R.G.V., Ouzman, J. and Boss, P.K. (2011). Variation in vine vigour, grape yield and vineyard soils and topography as indicators of variation in the chemical composition of grapes, wine and wine sensory attributes. *Australian Journal of Grape and Wine Research*, *17*, 217-229.

Burrough, P.A. and McDonnell, R.A. (1998). *Principles of Geographical Information Systems*, 2nd ed.; Oxford University Press: New York, USA, p. 333

Callegary, J.B., Ferre, T.P.A. and Groom, R.W. (2007). Vertical spatial sensitivity and exploration depth of low-induction-number electromagnetic-induction instruments. *Vadose Zone Journal, 6(1)*, 158-167

CEMA-European Agricultural Machinery Association. http://www.cema-agri.org/page/global-food-challenge

Cilia, C., Panigada, C., Rossini, M., Meroni, M., Busetto, L., Amaducci, S., Boschetti, M., Picchi, V. and Colombo, R. (2014). Nitrogen Status Assessment for Variable Rate Fertilization in Maize through Hyperspectral Imagery. Remote Sens., 6, 6549-6565

Cohen Y., Alchanatis V., Meron M., Saranga Y. and Tsipris J. (2005). Estimation of leaf water potential by thermal imagery and spatial analysis. *Journal of Experimental Botany, 56*, 1843-1852

Corwin, D.L. and Lesch, S.M. (2005). Characterizing soil spatial variability with apparent soil electrical conductivity: I. Survey protocols. *Computers and Electronics in Agricultura*, *46*, 103-133

Cox, P.G. (1996). Some issues in the design of agricultural decision support system. *Agricultural Systems*, *52 (2-3)*, 355-381

Dancey, C. and Reidy, J. (2004). *Statistics without Maths for Psychology: Using SPSS for Windows*; Prentice Hall: London, UK

DeJonge, K.C., Taghvaeian, S., Trout, T.J. and Comas, L.H. (2015). Comparison of canopy temperature-based water stress indices for maize. *Agricultural Water Management*, *156*, 51-62

Delefortrie, S., Saey, T., Van De Vijver, E., De Smedt, P., Missiaen, T., Demerre, I. and Van Meirvenne, M. (2014). Frequency domain electromagnetic induction survey in the intertidal zone: Limitations of low-induction-number and depth of exploration. *Journal of Applied Geophysics, 100*, 14-22

Demmel, M. (2013). Site-Specific Recording of Yields*. In Precision in Crop Farming: Site-Specific Concepts and Sensing Methods; Applications and Results*; Heege, H.J., Ed.; Springer: Kiel, Germany; Volume XI, p. 356

Demmel, M. (2001). Yield recording in combines-yield determination for site-specific yield sensing. DLG Merkblatt 303. Hrsg: Deutsche Landwirtschafts-Gesellschaft, Fachbereich Landtechnik, Ausschuss für Arbeitswirtschaft und Prozesstechnik, Deutsche Landwirtschafts-Gesellschaft; 1-20. (In German)

Drechsel, P., Heffer, P., Magen, H., Mikkelsen, R. and Wichelns, D. (2015). *Managing water and fertilizer for sustainable agricultural intensification*. IWMI Books, Reports

Dubovyk, O. (2017) The role of Remote Sensing in land degradation assessments: opportunities and challenges, European Journal of Remote Sensing, 50:1, 601-613

Egea, G., Nortes, P.A., Domingo, R., Baille, A., Pérez Pastor, A. and González-Real, M.M. (2013). Almond agronomic response to long-term deficit irrigation applied since orchard establishment. *Irrigation Science, 31*, 445-454

Eghball, B., Schepers, J.S., Negahban, M and Schlemmer, R.S. (2003). Spatial and temporal variability of soil nitrate and corn yield. *Soil Science Society of America Journal, 95(2)*, 339-346

European Parliament. Science and Technology Options Assessment, 2nd. STOA Options Brief-Plant breeding and innovative agriculture; available at http://www.europarl.europa.eu/stoa/cms/home/events/workshops/feeding

Eurostat-European Statistics. https://ec.europa.eu/eurostat

Evans, E.J., Shield, R.S. and Mohamed, S.B. (1997). Optimisation of Lime Application to Take Account of Within Field Variation in pH and Soil Texture*.* In *Proceedings of the first European Conference on Precision Agriculture,* Warwick University Conference Centre, Coventry, UK, 7–10 September 1997; pp. 95–103

Fabeiro, C., Martin de Santa Olalla, C., Lopez, R. and Dominguez, A. (2003). Production and quality of the sugar beet (Beta vulgaris L.) cultivated under controlled deficit irrigation conditions in a semi-arid climate. *Agricultural Water Management, 62*, 215-227

Fao-Food and Agriculture Organization. www.fao.org

Fundación Aquae. www.fundacionaquae.org

Ginestar, C. and Castel, J.R. (1996). Responses of young clementine citrus trees to water stress during different phonological periods. *Journal of Horticultural Science, 71*, 551-559

Gonzalez-Dugo, M.P., Moran, M.S., Mateos, L. and Bryant, R. (2006). Canopy temperature variability as an indicator of crop water stress severity. *Irrigation Science*, *24*, 233-240

González-Fernández, P. (2004). La fertilidad de los suelos y el abonado en la agricultura de conservación. In *Técnicas de Agricultura de Conservación*; Gil-Ribes, J., Blanco, G., Rodríguez-Lizana, A., Eds.; Mundi-Prensa: Madrid, Spain

Goovaerts, P. (1998). Geostatistical tools for characterizing the spatial variability of microbiological and physico-chemical soil properties. *Biol Fertil Soils, 27(4)*, 315-334

Goovaerts, P. (1997). Geostatistics for natural resources evaluation. In *Applied Geostatistics Series*. New York: Oxford University Press

Grisso, R.D, Alley, M.M., Thomason, W.E., Holshouser, D.L. and Roberson, G.T. (2011). Precision farming tools: variable-rate application. *Virginia Cooperative Extension* 442-505

Gutiérrez-Soto, M.V., Cadet-Piedra, E., Rodríguez-Montero, W. and Araya-Alfaro, J.M. (2011). GreenSeeker and the diagnosis of crop health. *Agron. Mesoam*, *22,* 397–403

Hall, D.K., Riggs, G.A., Salomonson, V.V., DiGirolamo, N.E. and Bayr, K.J. (2002). MODIS snow-cover products. *Remote Sens. Environ*. *83,* 181-194

Hall, A., Lamb, D.W., Holzapfel, B. and Louis J. (2008). Optical remote sensing applications in viticulture - a review. *Australian Journal of grape and Wine Research 8*, 36-47

Huete, A., Didan, K., Shimabokuro, Y., Ferreira, L. and Rodriguez E. (2000). Regional amazon basin and global analyses of MODIS vegetation indices: Early results and comparisons with AVHRR. International Geoscience and Remote Sensing Symposium (IGARSS) 2, pp. 536-538

Hummel, R.E. and Guenther, K.H. (1995). *Handbook of optical properties: thin films for optical coatings*. Crc Press.

Idso, S.B. (1982). Non-water stressed baselines: a key to measuring and interpreting plant water stress. *Agriculture Meteorology, 27*, 59-70

Idso, S.B., Jackson, R.D., Pinter, P.J., Reginato, R.J. and Hatfield, J.L. (1981). Normalizing the stress-degree-day parameter for environmental variability. *Agriculture Meteorology, 24*, 45-55

Jackson, R.D., Idso, S.B., Reginato, R.J., and Pinter, P.J. (1981). Canopy temperature as a crop water-stress indicator. *Water Resources Reseach, 17*, 1133-1138

Janssen, B.H., Guiking, F.C.T., Van der Eijk, D., Smaling, E.M.A., Wolf, J. and Van Reuler, H. (1990). A system for quantitative evaluation of the fertility of tropical soils (QUEFTS). *Geoderma, 46*, 299–318

Jones, H.G. (1992). *Plants and microclimate*. (2nd ed.) Cambridge: Cambridge University Press

Jones, H.G. (2004). Irrigation scheduling: advantages and pitfalls of plant-based methods. *Journal of Experimental Botany, 55*, 2427-2436

Käthner, J., Ben-Gal, A., Gebbers, R., Peeters, A., Herppich. W. B., and Zude-Sasse, M. (2017). Evaluating Spatially Resolved Influence of Soil and Tree Water Status on Quality of European Plum Grown in Semi-humid Climate. *Frontiers in Plant Science*, *8*, 1053

Krishna, K.R. (2016). *Push button agriculture: Robotics, drones, satellites-guided soil and crop management*. Oakville (Canada): Apple Academic Press, Inc

Liu, M., Yu, Z., Liu, Y. and Konijn, N.T. (2006). Fertilizer requirements for wheat and maize in China: The QUEFTS approach. *Nutr. Cycl. Agroecosyst.*, *74*, 245-258

López-Moreno, J.I., Vicente-Serrano, S.M., Beguería, S., García-Ruiz, J.M., Portela, M.M. and Almeida, A.B. (2009). Dam effects on droughts magnitude and

duration in a transboundary basin: The lower River Tagus, Spain and Portugal. *Water Resources Research, 45*, W02405

Lunetta, R.S., Johnson, D.M., Lyon, J.G. and Crotwell, J. (2004). Impacts of imagery temporal frequency on land-cover change detection monitoring. *Remote Sensing of Environment*, *89*, 444-454

Maes, W.H. and Steppe, K. (2012). Estimating evapotranspiration and drought stress with ground-based thermal remote sensing in agriculture: a review. *Journal of Experimental Botany, 63*, 4671-4712

Magrama-Ministerio de Agricultura, Alimentación y Medio Ambiente. Available online: http://www.magrama.gob.es/es/

Mapa-Ministerio de Agricultura, Pesca y Alimentación. https://www.mapa.gob.es/es/agricultura/temas/producciones-agricolas/cultivos-herbaceos/remolacha-azucarera/default.aspx

Mapa-Ministerio de Agricultura, Pesca y Alimentación. https://www.mapa.gob.es/es/agricultura/temas/producciones-agricolas/cultivos-herbaceos/cereales/

Martínez-Casasnovas, J.A., Agelet-Fernandez, J., Arno, J. and Ramos M.C. (2012). Analysis of vineyard differential management zones and relation to vine development, grape maturity and quality. *Spanish Journal of Agricultural Research 10(2),* 326-337

Massey Ferguson (1993). Yield Mapping System. Manufacturer's Catalog. MF 30/40 Series Combines.

McNeill, J.D. (1980). *Electromagnetic terrain conductivity measurement at low induction numbers*. Technical Note TN-6. Mississauga, ON, Canada: Geonics Ltd

Mills, H. and Jones, J.B. (1996). *Plant Analysis Handbook II: A Practical Sampling, Preparation, Analysis, and Interpretation Guide*; Micro-Macro Publishing, Inc.: Athens, GA, USA

Miller M.P., Singer, M.J. and Nielsen, D.R. (1988). Spatial Variability of Wheat Yield and Soil Properties on Complex Hills. *Soil Science Society of America Journal, 52(4)* 1133-1141

Möller, M., Alchanatis, V., Cohen, Y., Meron, M., Tsipris, J., Naor, A., Ostrovsky, V., Sprintsin, M. and Cohen, S. (2007). Use of thermal and visible imagery for estimating crop water status of irrigated grapevine. *Journal of Experimental Botany, 58*, 827-838

Moral, F.J., Terrón, J.M., Rebollo, J.F. (2010). Site-specific management zones based on the Rasch model and geostatistical techniques. *Computers and electronics in agriculture, 75*, 223-230

Müller, H., Rufin, P., Griffiths, P., Barros Siqueira, A.J. and Hostert, P (2015). Mining dense Landsat time series for separating cropland and pasture in a heterogeneous Brazilian savanna landscape. *Remote Sensing of Environment, 156, 223-230*

Myers, B.J. (1988). Water stress integral-a link between short-term stress and long-term growth. *Tree Physiology*, *4*, 315-323

Oksanen, T. (2013). Estimating Operational Efficiency of Field Work Based on fields shape. *In Proceedings of the 4th IFAC Conference on Modelling and Control in Agriculture, Horticulture and Post Harvest Industry,* Aalto University, Espoo, Finland, 28-29 August 2013; pp. 202–206

O'Shaughnessy, S.A., Steven R.E. and Paul D.C. (2015). Dynamic prescription maps for site-specific variable rate irrigation of cotton. *Agricultural Water Management, 159*, 123-138

Payero J.O., Tarkalson, D. and Irmak, S. (2006). *Corn yield response to different irrigation depths with subsurface drip irrigation*. Omaha, Nebraska: World Environmental and Water Resources Congress 2006

Pedrera-Parrilla, A. (2014). Integración de múltiples señales de sensores geofísicos para explorar el suelo a escala de cuenca agrícola (Tesis doctoral). Universidad de Córdoba.

Pedroso, M., Taylor, J., Tisseyre, B., Charnomordic, B. and Guillaume, S. (2010). A segmentation algorithm for the delineation of agricultural management zones. *Comput. Electron. Agric.*, *70*, 199-208

Pedersen, S.M. and Lind, K.M. (2017). *Precision Agriculture: Technology and Economic Perspectives*. Springer-Verlag GmbH

Peña, J.M., Torres-Sánchez, J., de Castro, A.I., Kelly, M. and López-Granados, F. (2013). Weed mapping in early-season maize fields using object-based analysis of unmanned aerial vehicle (UAV) images. *PLoS One*, *8*

Qi, Z. & Helmers, M.J. (2010). The conversion of permittivity as measured by a PR2 capacitance probe into soil moisture values for Des Moines lobe soils in Iowa. *Soil Use and Management*, 26, 82-92

R Core Team. (2014). R: A language and environment for statistical computing. In *R Foundation for Statistical Computing*; Vienna, Austria. Available online: http://www.R-project.org/

Raun, W.R. and Johnson, G.V. (1999). Improving nitrogen use efficiency for cereal production. *Agronomy Journal*, *91*, 57-351

Raun, W.R., Solie, J.B., Stone, M.L, Martin, K.L., Freeman, K.W., Mullen, R.W., Zhang, H., Schepers, J.S. and Johnson, G.V (2005). Optical sensor-based algorithm for crop nitrogen fertilization, Communications in *Soil Science and Plant Analysis*, *36*, 2759-2781

Rouse, J.W., Haas, R.W., Schell, J.A., Deering, D.W. and Harlan, J.C. (1974). *Monitoring the vernal advancement and retrogradation (Green-wave effect) of natural vegetation.* NASA/GSFC Type III Final Report Greenbelt, MD, USA

Rud, R., Cohen, Y., Alchanatis, V., Beiersdorf, I., Klose, R.and Presnov, E. et al. (2015). Characterization of salinity-induced effects in olive trees based on thermal imagery. In *Precision Agriculture* - Pap. Present. 10th Eur. Conf. Precis. Agric. ECPA 2015 (pp 511-518)

Rud, R., Cohen, Y., Alchanatis, V., Levi, A., Brikman, R., Shenderey, C., et al. (2014). Crop Water Stress Index derived from multi-year ground and aerial thermal images as an indicator of potato water status. *Precision Agriculture*, 15, 273-289

Schaap, M.G., Leij, F.J. and Van Genuchten, M. Th. (1999). A bootstrap-neural network approach to predict soil hydraulic parameters. In: Van Genuchten, M.Th., Leij, F.J. & Wu, L. (eds), Proc. Int. Workshop, *Characterization and Measurements of the Hydraulic Properties of Unsaturated Porous Media*, pp 1237-1250, University of California, Riverside, CA.

Schepers, A.R., Shanahan, J.F., Liebig, M.A., Schepers, J.S., Johnson, S.H. and Luchiari A. (2004). Appropriateness of management zones for characterizing spatial variability of soil properties and irrigated corn yields across years. *Soil Science Society of America Journal, 96(1*), 195-203

Scholander, P.F., Hammel, H.T., Bradstreet, E.D. and Hemmingsen, E.A. (1965). Sap pressure in vascular plants. *Science*, *148*, 339-346

Searcy, S. W., Schueller, J. K., Base, Y. H., Borgelt, S. C. and Stout, B. A. (1989). Mapping of spatially variable yield during grain combining. *Transactions of the ASAE 32(3)*, 826–829

Shanahan, J.F., Kitchen, N.R., Raun, W.R. and Schepers, J.S. (2008). Responsive in season nitrogen management for cereals. *Comput. Electron. Agric.*, *61*, 51-62

Simpson, D., Van Meirvenne, M., Saey, T., Vermeersch, H., Bourgeois, J., Lehouck, A., Cockx, L. and Vitharana, U.A. (2009). Evaluating the multiple coil configurations of the EM38DD and DUALEM-21S sensors to detect archaeological anomalies. *Archaeol. Prospect, 16*, 91-102

Snyder, W. and Wan, Z. (1998). BRDF models to predict spectral reflectance and emissivity in the thermal infrared. *IEEE Transactions on Geoscience and Remote Sensing*, *36(1)*, 214-225

Sobrino, J.A., Raissouni, N., Kerr, Y., Olioso, A., López-García, M.J., Belaid, A., El Kharraz, M.H., Cuenca, J. and Dempere, L. (2000) *Teledetección*; Sobrino, J.A., Ed.; Universidad de Valencia: Valencia, Spain

Sugiura, R., Noguchi, N. and Ishii, K. (2007). Correction of Low-altitude Thermal Images applied to estimating Soil Water Status. *Biosystems Engineering, 96*, 301-313

Stamatiadis, S., Tsadilas, C. and Schepers, J.S. (2010). Ground-based canopy sensing for detecting effects of water stress in cotton. *Plant Soil*, *331*, 277-287

Taghvaeian S., Comas L., DeJonge K.C. and Trout T.J. (2014). Conventional and simplified canopy temperature indices predict water stress in sunflower. *Agriculture Water Management, 144*, 69-80

Tarpley, L., Reddy, K.R. and Sassenrath-Cole, G.F. (2000). Reflectance indices with precision and accuracy in predicting cotton leaf nitrogen concentration. *Crop Science*, *40*, 1814-1819

Testi, L., Goldhamer, D.A., Iniesta, F. and Salinas, M. (2008). Crop water stress index is a sensitive water stress indicator in pistachio trees. *Irrigation Science, 26*, 395-405

Thomasson, J.A. and Sui, R. (2009). Cotton leaf reflectance changes after removal from the plant. *Journal of Cotton Science*, *13*, 183-188

Vansichen, R. and De Baerdemaeker, J. (1991). Continous wheat yield measurement on a combine. In: *Automated Agriculture for the 21st Century*. American Society of Agricultural Engineers, St. Joseph, Mich., ASAE-Publ., 11-91: 346-355.

Van der Burgt, G.J.H.M., Oomen, G.J.M., Habets, A.S.J. and Rossing, W.A.H. (2006). The NDICEA model, a tool to improve nitrogen use efficiency in cropping Systems. *Nutr. Cycl. Agroecosyst.*, *74*, 275-294

Van Genuchten, M.T. (1980). A closed-form equation for predicting the hydraulic conductivity of unsaturated soils. *Soil Science Society of America Journal, 44*, 892-898

Verhoef, A. and Egea, G. (2013). Soil water and its management. In: Gregory, P.J. & Nortcliff, S. (Eds.), *Soil conditions and plant growth*. Wiley-Blackwell, West Sussex, UK. 461 p.

Wang, Y., Zia, S., Owusu-Adu, S., Gerhards, R. and Müller, J. (2014). Early detection of fungal diseases in winter wheat by multi-optical sensor. *Procedia APCBEE*, *8*, 199-203

Wheeler, T.R., Batts, G.R., Ellis, R.H., Hadley, P. and Morison, J.I.L. (1996). Growth and yield of winter wheat (*Triticum aestivum*) crops in response to CO_2 and temperature. *Journal of Agricultural Sci*ence, *127*, 37-48

Wild, A. (1992). Elementos nutritivos en el suelo: Nitrógeno. In *Condiciones del Suelo y Desarrollo de las Plantas Según Russell*; En Wild, A., Ed.; Mundi-Prensa: Madrid, Spain

Yang, C., Everitt, J.H. and Bradford, J.M. (2006). Comparison of QuickBird satellite imagery and airborne imagery for mapping grain sorghum yield patterns. *Precision Agriculture*, *7*, 33-44

Zarco-Tejada, P.J., Whiting, M. and Ustin, S.L. (2005). Temporal and Spatial relationship between whithin-field yield variability in cotton and high spatial hyperspectral remote sensing imagery. *Agronomy Journal*, *97*, 641-653

Zhang, D., Zhou, X., Zhang, J., Lan, Y., Xu, C. and Liang D. (2018). Detection of rice sheath blight using an unmanned aerial system with high-resolution color and multispectral imaging. PLoS ONE 13(5): e0187470

Zhang, L., Clarke, M.L., Steven, M.D. and Jaggard, K.W. (2011). Spatial patterns of wilting in sugar beet as an indicator for precision irrigation. *Precision Agriculture*, *12*, 296-316

Zude-Sasse, M., Fountas, S., Gemtos, T.A. and Abu-Khalaf, N. (2016). Applications of precision agriculture in horticultural crops. *European Journal of Horticultural Science, 81(2)*, 78-90

Appendix

Research contribution

This thesis is a compendium of articles, including two articles published in impact scientific journals and in which the author has been involved (JCR (SCI) indexed journals).

The author has been involved in these papers and is listed as the first author in both papers but as the articles have been published in collaboration with other co-authors the contribution is indicated in each of them:

- **Publication 1:** *"An approach to precise Nitrogen management using hand-held crop sensor measurements and winter wheat yield mapping in a Mediterranean Environment"*

Contributions of the PhD candidate:

- Analysis of the problem and bibliographical study of the state of the art

- Design and conducting field experiments

- Analysis of results and data processing with GIS

- Preparation, drafting and review of the article

- **Publication 2:** *"Linking thermal imaging and soil remote sensing to enhance irrigation management of sugar beet"*

- Analysis of the problem and bibliographical study of the state of the art

- Planning and execution of field experiments

- Analysis of results and data processing with GIS

- Preparation, drafting and review of the article

- Other publications by the author:

The author has other contributions to the scientific community in articles in technical journals specialized in the agrarian sector, contributions in national and international congresses, etc.

Articles in non JCR (SCI) indexed journals:

- Pérez-Ruiz, M, Egea, G., **Quebrajo, L**., Martínez, J. (2015) Los "drones agrícolas" son el principal avance tecnológico en 2014. *Tierras de Castilla y León: Agricultura, 224*, 44-54

- Egea, G., **Quebrajo Moya, L**., Martínez, J., Pérez-Urrestarazu, L., Bermejo, J.L., Pérez-Ruiz, M. (2016). Uso de imágenes térmicas aéreas en remolacha azucarera para propuesta de riego de precisión. *Aimcra Asociación de investigación para la mejora del cultivo de la remolacha azucarera, 125*, 21-24

Congresses:

- Pérez-Ruiz, M., Agüera Vega, J. Rodriguez Lizana, A. **Quebrajo Moya, L.** *"Understanding hand-held crop sensor measurements and winter wheat yield mapping in the Mediterranean environment"*. 10th European Conference on Precision Agriculture. July 2015 Volcani Center, Israel

- **Quebrajo Moya, L.**, Egea, G., Pérez-Ruiz, M. y Pérez-Urrestarazu, L. *"Uso de imágenes térmicas aéreas en remolacha azucarera (Beta vulgaris) para propuesta de riego de precisión"*. XXXIV Congreso Nacional de Riego. Junio 2016 Sevilla, España

Book:

- Manuel Pérez-Ruíz, **Lucía Quebrajo Moya**, Jorge Martínez Guanter y Juan Agüera Vega. (2015). *Introducción a la agricultura de precisión en el Valle del Guadalquivir*. Sevilla. ISBN 978-84-608-2673-6

Newspaper coverage:

- News in the economy section of "El correo de Andalucía" on 17 June 2014

El Correo de Andalucía

ECONOMÍA 33

MALA HIERBA A VISTA DE 'DRON'

Un grupo de investigación de la Universidad de Sevilla desarrolla un vehículo aéreo no tripulado que detecta con infrarrojos las plantas no deseadas para aplicar los herbicidas exclusivamente en la zona señalada

El equipo de investigación que lidera el profesor Manuel Pérez, tercero por la izquierda, haciendo un trabajo de campo.

El vehículo aéreo no tripulado trabaja con rayos infrarrojos.